# The bead model & limit behaviors of dimer models

Cédric Boutillier[*]

8th February 2008

**Abstract**

In this paper, we study the *bead model*: beads are threaded on a set of wires on the plane represented by parallel straight lines. We add the constraint that between two consecutive beads on a wire, there must be exactly one bead on each neighboring wire. We construct a one-parameter family of Gibbs measures on the bead configurations that are uniform in a certain sense. When endowed with one of these measures, this model is shown to be a determinantal point process, whose marginal on each wire is the *sine process* (given by eigenvalues of large hermitian random matrices). We prove then that this process appears as a limit of any dimer model on a planar bipartite graph when some weights degenerate.

## 1  Introduction and presentation of the bead model

We consider the collection of configurations of beads strung on an infinite collection of parallel threads lying on the plane. A bead configuration on these threads gives a configuration of points on $\mathbb{Z} \times \mathbb{R}$. We impose the following constraints on the configurations:
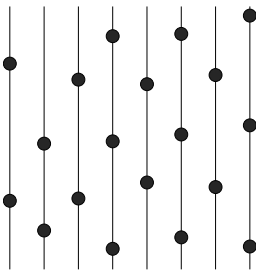


Figure 1: A bead configuration.

- The configuration must be locally finite : the number of beads in each finite interval of a thread must be finite.

---

[*]Centrum voor Wiskunde en Informatica - P.O. Box 94079, NL-1090 GB Amsterdam
`cedric.boutillier@cwi.nl`

- Between two consecutive beads on a thread, there must be exactly one bead on each neighboring thread.

Let $\Omega$ be the set of bead configurations satisfying these two conditions.

The first aim of this paper is to construct probability measures for our infinite system $\Omega$ that are uniform in a certain sense.

If there were only a finite number of threads of finite length, and a fixed number of beads on each thread, then the set $\Omega$ would be a bounded convex set of $\mathbb{R}^N$, where $N$ is the total number of beads. Therefore the normalized Lebesgue measure on $\Omega$ would give a uniform probability measure. Therefore we look for probability measures that satisfy the two following properties:

- they are ergodic under the action of $\mathbb{Z} \times \mathbb{R}$ by translation

- conditioned in an annular region, they induce the uniform measure on allowed configurations inside this region.

Such a probability measure is called an *ergodic Gibbs measure*. When endowed with an ergodic Gibbs measure, the set $\Omega$ is called a *bead model*.

This model can be viewed as a interface model on $\mathbb{Z}^2$. Indeed, the position of the beads have the same combinatorics as the square lattice $\mathbb{Z}^2$ (rotated counterclockwise by $\pi/4$). A configuration can therefore encoded by a *height function* $\phi : \mathbb{Z}^2 \to \mathbb{R}$, where $\phi(x, y)$ is the ordinate of the bead $(x, y)$ on its thread. The problem of existence (and uniqueness) of Gibbs measures for this model can thus be formulated in terms of *random surfaces with a simple attractive potential* [15] reflecting the hard-core interaction between beads. However, this approach does not lead to an explicit expression for the Gibbs measures. We adopt another point of view that will allows us to give a closed formula for cylinder events.

The $\sigma$-algebra of events for our probability measures is defined as follows. To each bounded Borel set $B$ of $\mathbb{Z} \times \mathbb{R}$ and to each bead configuration $\omega \in \Omega$ is associated an integer $X_B(\omega)$. Let $\mathcal{F}$ be the smallest $\sigma$-algebra such that all the maps $X_B : \Omega \to \mathbb{N}$ are measurable. $\mathcal{F}$ is generated by the elementary events

$$\big\{ \omega \in \Omega \mid X_B(\omega) = n \big\}.$$

If $\mathbb{P}$ is a Gibbs measure on $(\Omega, \mathcal{F})$, it defines through the application $X : B \mapsto X_B$ a random process with value in the set of boundedly finite, integer-valued measures, *i.e.* in other words, a *random point field*.

Even without giving for the moment any explicit description for a Gibbs measure, it is possible to estimate, at least heuristically, the probability of rare events. For example, one can estimate the probability that $n$ beads lie in the same wire interval of length $\varepsilon$. For this event to occur, then, due to the geometrical constraint imposed on configurations, there must be $n-1$ beads in a small interval of size $\varepsilon$ on the left neighbor thread, and $n-2$ beads in the same interval on its left, and so on, and the same must happen on the the right side of the considered thread. That is why the probability of this event must be of order $\varepsilon^{n+2\sum_{k=1}^{n-1}(n-k)} = \varepsilon^{n^2}$. Note that this is much smaller than the probability of having $n$ points of a *Poisson process* in such a small interval, which is of order $\varepsilon^n$: there is thus a kind of repulsion between beads, induced by the geometrical constraint on bead configurations.

Such a repulsion has been observed in some point processes on the real line, especially in *determinantal point processes* [16], for which correlation functions are expressed as determinants of a certain kernel. Certainly, the most famous example of such processes is the so-called *sine process*,

which describes the statistics of the eigenvalues of large random hermitian matrices with Gaussian entries (GUE ensemble [10]) in the bulk of the spectrum, and whose kernel is given by he following expression:

$$k(x, y) = \frac{\sin(x - y)}{\pi(x - y)}.$$

We will see that the Gibbs measures we construct on $(\Omega, \mathcal{F})$ define determinant random point fields on $\mathbb{Z} \times \mathbb{R}$, for which correlations functions are given by determinants of a kernel $J$, whose restriction to a single thread is the sine kernel.

We prove the following theorem:

**Theorem 1.** *For a fixed average density of beads, there exists a 1-parameter family of ergodic Gibbs measures $(\mathbb{P}_\gamma)$ on $(\Omega, \mathcal{F})$. When endowed with one of these measures, $(\Omega, \mathcal{F})$ is a determinantal random point field on $\mathbb{Z} \times \mathbb{R}$, and the probability of any cylinder event has a completely closed form. In particular, the marginal on each thread is the sine random point field.*

The exact expression for the kernel is given in Theorem 2. The parameter is directly related to the average distance between a bead and its right neighbor just below it and describes the amplitude of a magnetic field that tends to push the beads in some directions.
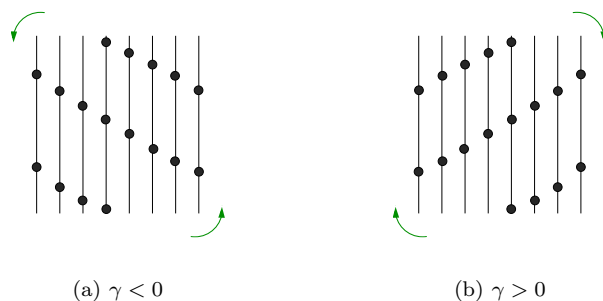


(a) $\gamma < 0$          (b) $\gamma > 0$

Figure 2: Two typical bead configurations for different values of $\gamma$. The parameter $\gamma$ is negative in panel (a), and positive in panel (b).

A way to construct these Gibbs measures is first to consider a discretized version of the bead model. The set of possible configurations $\Omega_{\mathtt{t}} \subset \Omega$, is constituted by the configurations for which the beads are located at sites of a lattice with mesh $\mathtt{t}$. We show in sections 2 and 3 that in this discrete setting, there exist probability measures supported by $\Omega_{\mathtt{t}}$, for which the distribution of the beads is a determinantal random point field, by exhibiting a bijection between the discretized bead model and the dimer model on the honeycomb lattice — or equivalently random tilings of the plane by rhombi. The measures on random tilings have the Gibbs property. Then we prove that the sequence of discrete determinantal processes indexed by $\mathtt{t}$ converges to a determinantal random point field on $\mathbb{Z} \times \mathbb{R}$ when $\mathtt{t}$ goes to zero. In the second part of the paper (section 5 and 6), we prove that the bead model appears not only as a limit of the dimer model on the honeycomb lattice, but as the universal limit behavior of the dimer model on any bipartite periodic planar graph.

The fact that the correlations between dimers is given by the (discrete) sine kernel has been noticed before in particular cases by Johansson [5] and Baik *et al* [1]. Our approach gives a

3

systematic method to find a subset of edges, for which correlations can be made arbitrarily close to the sine process.

# 2 A discrete version of the bead model and the dimer model on the honeycomb lattice

We assume for the moment that the threads are not continuous lines, but a one-dimensional lattice with mesh size $\mathtt{t}$. The possible positions of the beads are labeled by coordinates

$$(x, \mathtt{t}y) \in \mathbb{Z} \times \mathtt{t}\mathbb{Z}, \tag{1}$$

$x$ representing the thread on which the bead lies, and $y$ being the coordinate running along the thread.

There is a mapping between discrete bead configurations and dimer configurations on the honeycomb lattice $H$. Before explaining this mapping, we recall some facts about the dimer model on $H$.

## 2.1 The dimer model on $H$

A *dimer configuration* of the honeycomb lattice $H$ is a subset of edges of $H$ such that every vertex is incident with exactly one edge of this subset. A dimer configuration is also called in graph theory a *perfect matching*. On the set of all possible dimer configurations, there is a two-parameter family [9] of *Gibbs probability measures*, all elements of which satisfy the following properties:

- They are ergodic under the action of the lattice translations $\mathbb{Z} \times \mathbb{Z}$,

- If a dimer configuration is fixed in an annular region of $H$, the dimer configurations on the inside and in the outside region are independent, and the dimer configurations inside are uniformly distributed.

Here is how these measures are defined, following [9, 6]. The vertices of $H$ are colored in white and black such that no two neighbors have the same color. Weights are assigned to edges of $H$ according to their orientation: $a$, $b$, $c$. A fundamental domain of $H$ is obtained by taking for example a white and a black vertex sharing an horizontal edge. The vertices of $H$ are labeled by their color and the coordinates of their fundamental domain $(x, y)$.

The local statistics for the Gibbs measure corresponding to these weights have a determinantal form: the probability that edges $\mathbf{e}_1 = (\mathbf{w}_{x_1,y_1}, \mathbf{b}_{x'_1,y'_1}), \ldots, \mathbf{e}_k = (\mathbf{w}_{x_k,y_k}, \mathbf{b}_{x'_k,y'_k})$ belong to the random dimer configuration are given by

$$\mathbb{P}\left[\mathbf{e}_1, \ldots, \mathbf{e}_k\right] = \left(\prod_{j=1}^{k} \mathsf{K}(\mathbf{w}_{x_j,y_j}, \mathbf{b}_{x'_j,y'_j})\right) \det_{1 \leq i,j \leq k} \left[\mathsf{K}^{-1}(\mathbf{b}_{x'_i,y'_i}, \mathbf{w}_{x_j,y_j})\right] \tag{2}$$

where $\mathsf{K}$ is the so-called *Kasteleyn operator*. In the case of the honeycomb lattice, it is simply the weighted adjacency matrix restricted to the lines corresponding to white vertices, and columns corresponding to black vertices: if $\mathbf{w}$ and $\mathbf{b}$ are neighbors, then $\mathsf{K}(\mathbf{w}, \mathbf{b}) = a$, $b$ or $c$ depending on

4

the orientation of the edge $(\mathbf{w}, \mathbf{b})$. If they are not neighbors, then $\mathsf{K}(\mathbf{w}, \mathbf{b}) = 0$. Since $\mathsf{K}$ is $\mathbb{Z}^2$ periodic, its inverse can be expressed using inverse Fourier transform over the unit torus:

$$\mathsf{K}^{-1}(\mathbf{b}_{x',y'}, \mathbf{w}_{x,y}) = \mathsf{K}^{-1}(\mathbf{b}_{(x'-x),(y'-y)}, \mathbf{w}_{0,0}) = \iint_{\mathbb{T}^2} \frac{z^{-(y'-y)} w^{(x'-x)}}{a + b/w + cz/w} \frac{\mathrm{d}z}{2i\pi z} \frac{\mathrm{d}w}{2i\pi w}. \tag{3}$$

When none of the weights is greater than the sum of the other two, one can show (by computing explicitly the integral above) that every type of edge appears in the random dimer configuration with positive probability. The measure is then said to be *liquid* [9].

For such weights, there is particularly well-adapted embedding for the hexagonal lattice, the so-called *isoradial embedding* [7] corresponding to these weights, defined as follows: the length of a dual edge of $H$ is equal to the weight of the corresponding primal edge, so that the dual faces of $H$ are represented as triangles with side length $a$, $b$ and $c$. The dual faces for the usual embedding of $H$ with regular hexagons are equilateral triangles and the this embedding corresponds to equally distributed weights $a = b = c$.

The measure and the embedding (up to a global scaling factor) depend only on the ratios $a/b$ and $c/b$. For our purpose, we will chose $a = \mathsf{t}$, $b = 1$, and $c = \exp(\gamma\mathsf{t})$. These values satisfy the triangular inequalities for $\gamma \in (-1, 1)$ at least for $\mathsf{t}$ small enough. The distance between two successive horizontal edges is $\mathsf{t}$. We denote by $\mathbb{P}_{\gamma,\mathsf{t}}$ and $\mathsf{K}^{-1}_{\gamma,\mathsf{t}}$ the probability measure and the inverse Kasteleyn operator corresponding to these particular weights.

## 2.2 Correspondence between beads and dimers

The mapping we construct between discrete bead configurations and dimer configurations can be described as follows: there is a bead at $(x, \mathsf{t}y)$ if and only if the horizontal edge incident with the white vertex in fundamental domain $(x, y)$ is in the dimer configuration.

A way to see geometrically this correspondence is using these isoradial embeddings of the honeycomb lattice described above. Take an isoradial embedding of the honeycomb lattice for weights $a = \mathsf{t}$, $b = 1$, $c = e^{\gamma\mathsf{t}}$ for $\gamma \in (-1, 1)$. Once chosen a dimer configuration on $H$, draw a bead in the middle of an horizontal edge if it appears in the dimer configuration and you end with a discrete bead configuration with mesh size $\mathsf{t}$. Reciprocally, from a bead configuration one can reconstruct a dimer configuration by placing horizontal dimers on edges crossing an occupied site, and completing the configuration. This is always possible, because of the intertwining of bead positions. Moreover, the completion is unique as soon as there is at least one bead on each wire.

For a fixed $\mathsf{t}$, each value of $\gamma$ corresponds to a liquid Gibbs probability measure on dimer configurations, that can be transported to bead configurations. The local statistics of the beads coincide with that of horizontal dimers. The probability measure on bead configurations benefits from the conditional uniform property of the dimer Gibbs measure.

This procedure defines for a given $\mathsf{t}$ a family parameterized by $\gamma$ of probability measures on discrete bead configurations that have the conditioned uniform property. The correlations between beads are given by determinants: the probability of having a bead at the sites $(x_1, \mathsf{t}y_1), \ldots, (x_k, \mathsf{t}y_k)$ in the random bead configuration $\omega$ is

$$\mathbb{P}_{\gamma,\mathsf{t}}\left[(x_1, \mathsf{t}y_1), \ldots, (x_k, \mathsf{t}y_k) \in \omega\right] = t^k \det_{1 \leq i,j \leq k} \mathsf{K}^{-1}_{\gamma,\mathsf{t}}(\mathbf{b}_{x_i,y_i}, \mathbf{w}_{x_j,y_j}) \tag{4}$$
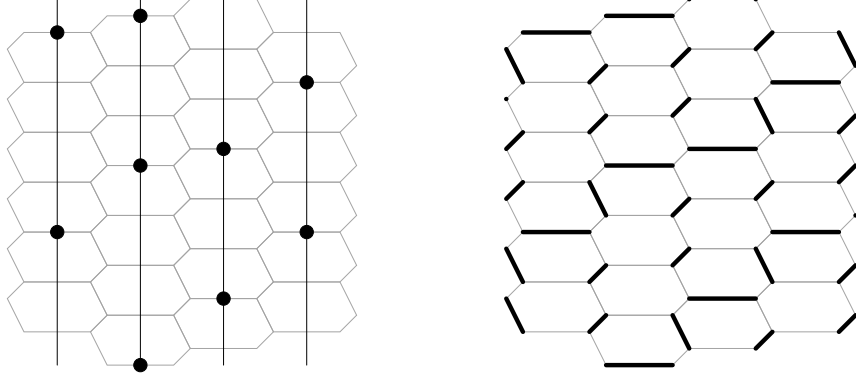
Figure 3: A piece of discrete bead configuration and the corresponding piece of dimer configuration on $H$.

where $\mathsf{K}_{\gamma,\mathsf{t}}^{-1}$ is defined by

$$\mathsf{K}_{\gamma,\mathsf{t}}^{-1}(\mathbf{b}_{x,y},\mathbf{w}) = \iint_{\mathbb{T}^2} \frac{z^{-y}w^x}{\mathsf{t} + \frac{1}{w}(1 + ze^{\gamma\mathsf{t}})} \frac{\mathrm{d}z}{2i\pi z} \frac{\mathrm{d}w}{2i\pi w} \tag{5}$$

# 3 Construction of explicit Gibbs measures for the continuous bead model

In this section, we will give an explicit description for Gibbs measures for the bead model. But before proving theorem 1, it is necessary to investigate the behavior of the kernel defining the discrete bead model. In other words, one has to compute the asymptotics of $\mathsf{K}_{\gamma,\mathsf{t}}^{-1}(\mathbf{b}_y^x,\mathbf{w})$ when $\mathsf{t}$ becomes small and $y$ large.

The first thing to note is that for the weights we chose, the probability of an horizontal edge at a given white vertex (that is the probability of a bead at a given site in the discrete model) is

$$\mathbb{P}_{\gamma,\mathsf{t}}[\text{horizontal edge}] = \mathsf{t}\mathsf{K}_{\gamma,\mathsf{t}}^{-1}(\mathbf{b}_{0,0},\mathbf{w}_{0,0}) = \mathsf{t}\iint_{\mathbb{T}^2} \frac{1}{\mathsf{t} + \frac{1}{w}(1 + ze^{\gamma\mathsf{t}})} \frac{\mathrm{d}z}{2i\pi z} \frac{\mathrm{d}w}{2i\pi w} = \mathsf{t}\sqrt{1-\gamma^2} + o(\mathsf{t}). \tag{6}$$

In order to keep a constant average density of beads, we must choose the rescaled vertical coordinate $\xi$ equal to $\mathsf{t}y\sqrt{1-\gamma^2}$.

The asymptotics of the kernel for this vertical scaling are given by the following lemma.

**Lemma 1.** *In the vertical scaling limit* $\mathsf{t} \to 0, \mathsf{t}y\sqrt{1-\gamma^2} \to \xi$, *the coefficients* $\frac{(-1)^y}{\sqrt{1-\gamma^2}}\mathsf{K}_{\gamma,t}^{-1}(\mathbf{b}_{x,y},\mathbf{w})$ *converge to*

$$J_\gamma(x,\xi) = \begin{cases} \displaystyle\int_{[-1,1]} e^{-i\xi\phi}(\gamma + i\phi\sqrt{1-\gamma^2})^x & \text{if } x \geq 0, \\ \displaystyle-\int_{\mathbb{R}\setminus[-1,1]} e^{-i\xi\phi}(\gamma + i\phi\sqrt{1-\gamma^2})^x \frac{\mathrm{d}\phi}{2\pi} & \text{if } x < 0. \end{cases} \tag{7}$$

6

*In particular, when $x = 0$,*

$$J_\gamma(0, \xi) = \frac{1}{2\pi} \int_{[-1,1]} e^{i\xi\phi} \mathrm{d}\phi = \frac{\sin(\xi)}{\pi\xi}. \tag{8}$$

*Proof.* As we said before, the entries of the inverse Kasteleyn operator are given by

$$\mathsf{K}_{\gamma,\mathsf{t}}^{-1}(\mathbf{b}_{x,y}, \mathbf{w}) = \iint_{\mathbb{T}^2} \frac{z^{-y}w^x}{\mathsf{t} + \frac{1}{w}(1 + ze^{\gamma\mathsf{t}})} \frac{\mathrm{d}z}{2i\pi z} \frac{\mathrm{d}w}{2i\pi w}$$

To evaluate this integral, we first perform the integration over $w$ by the method of residues. If $x \geq 0$, the rational fraction

$$f_z(w) = \frac{w^x}{\mathsf{t}w + (1 + ze^{\gamma\mathsf{t}})}$$

has one pole at $w = w_0(z) = -\frac{1+ze^{\gamma\mathsf{t}}}{\mathsf{t}}$.

By Cauchy's theorem, the integral

$$\frac{1}{2i\pi} \int_{\mathbb{S}^1} f_z(w) \mathrm{d}w$$

is zero unless the pole $w_0(z)$ is in the unit disc, *i.e.*

$$\mathrm{Re}(z) < -\frac{1 + e^{2\gamma\mathsf{t}} - \mathsf{t}^2}{2e^{\gamma\mathsf{t}}} = -1 + (1 - \gamma^2)\mathsf{t}^2 + O(\mathsf{t}^3). \tag{9}$$

Define $\theta_0 = \theta_0(\gamma, \mathsf{t}) = \mathrm{Arccos}\left(\frac{1+e^{2\gamma\mathsf{t}}-\mathsf{t}^2}{2e^{\gamma\mathsf{t}}}\right) = \mathsf{t}\sqrt{1-\gamma^2} + O(\mathsf{t}^2)$. The constraint (9) on the pole to be inside the unit disk can be rewritten as

$$\arg(z) \in (\pi - \theta_0, \pi + \theta_0)$$

Posing $z = -e^{i\theta} = -e^{i\mathsf{t}\phi\sqrt{1-\gamma^2}}$ in the integral, we get

$$\mathsf{K}_{\gamma,\mathsf{t}}^{-1}(\mathbf{b}_{x,y}, \mathbf{w}) = \int_{\mathrm{Re}(z) < -\frac{1+e^{2\gamma\mathsf{t}}-\mathsf{t}^2}{2e^{\gamma\mathsf{t}}}} z^{-y} \left(-\frac{1 + ze^{\gamma\mathsf{t}}}{\mathsf{t}}\right)^x \frac{\mathrm{d}z}{2\pi\mathsf{t}iz} \tag{10}$$

$$= (-1)^y \int_{-\theta_0}^{\theta_0} e^{-iy\theta} \left(\frac{e^{\gamma\mathsf{t}}e^{i\theta} - 1}{\mathsf{t}}\right)^x \frac{\mathrm{d}\theta}{2\pi\mathsf{t}} \tag{11}$$

$$= \frac{(-1)^y}{2\pi} \int_{-\theta_0/\mathsf{t}\sqrt{1-\gamma^2}}^{\theta_0/\mathsf{t}\sqrt{1-\gamma^2}} e^{-i\mathsf{t}y\phi} \left(\frac{e^{\mathsf{t}(\gamma+i\phi\sqrt{1-\gamma^2})} - 1}{\mathsf{t}}\right)^x \sqrt{1-\gamma^2}\mathrm{d}\phi. \tag{12}$$

In the vertical scaling limit $\mathsf{t} \to 0, \mathsf{t}y\sqrt{1-\gamma^2} \to \xi$, we have

$$\lim \frac{\theta_0}{\mathsf{t}\sqrt{1-\gamma^2}} = 1, \quad \lim e^{-i\mathsf{t}y\phi\sqrt{1-\gamma^2}} = e^{-i\xi\phi}, \quad \lim \frac{e^{\mathsf{t}(\gamma+i\phi\sqrt{1-\gamma^2})} - 1}{\mathsf{t}} = \gamma + i\phi\sqrt{1-\gamma^2}.$$

Thus, the integral above, multiplied by $\frac{(-1)^y}{\sqrt{1-\gamma^2}}$, converges to

$$\lim \frac{(-1)^y}{\sqrt{1-\gamma^2}} \mathsf{K}^{-1}(\mathbf{b}_{x,y}, \mathbf{w}) = \frac{1}{2\pi} \int_{[-1,1]} e^{-i\xi\phi} \left(\gamma + i\phi\sqrt{1-\gamma^2}\right)^x d\phi.$$

When $x < 0$, $f_z(w)$ has two poles: there is a pole at $w = 0$ in addition to that located at $w = w_0(z) = -\frac{1+ze^{\gamma t}}{t}$. Since $wf_z(w)$ goes to zero when $z$ goes to infinity, the sum of the residues is zero. Therefore the integral of $f_z(w)$ on the unit circle is not zero only if $w_0(z)$ is outside of the unit disc. It equals in that case the opposite of the residue at $w_0(z)$. Again with the change of variable $z = -e^{i\theta} = -e^{it\phi\sqrt{1-\gamma^2}}$, we have

$$\mathsf{K}_{\gamma,t}^{-1}(\mathbf{b}_{x,y}, \mathbf{w}) = -\int_{\mathrm{Re}(z) > -\frac{1+e^{2\gamma t}-t^2}{2e^{\gamma t}}} z^{-y} \left(-\frac{1 + ze^{\gamma t}}{t}\right)^x \frac{dz}{2\pi t i z} \tag{13}$$

$$= (-1)^{y+1} \left(\int_{-\pi}^{-\theta_0} + \int_{\theta_0}^{\pi}\right) e^{-iy\theta} \left(\frac{e^{\gamma t} e^{i\theta} - 1}{t}\right)^x \frac{d\theta}{2\pi t} \tag{14}$$

$$= (-1)^{y+1} \left(\int_{\frac{-\pi}{t\sqrt{1-\gamma^2}}}^{\frac{-\theta_0}{t\sqrt{1-\gamma^2}}} + \int_{\frac{\theta_0}{t\sqrt{1-\gamma^2}}}^{\frac{\pi}{t\sqrt{1-\gamma^2}}}\right) e^{-ity\phi\sqrt{1-\gamma^2}} \left(\frac{e^{\gamma t} e^{it\phi\sqrt{1-\gamma^2}} - 1}{t}\right)^x \frac{\sqrt{1-\gamma^2} d\phi}{2\pi}. \tag{15}$$

Thus in the scaling limit, by Lebesgue dominated convergence theorem,

$$\lim \frac{(-1)^y}{\sqrt{1-\gamma^2}} \mathsf{K}_{\gamma,t}^{-1}(\mathbf{b}_{x,y}, \mathbf{w}) = \frac{-1}{2\pi} \int_{\mathbb{R}\setminus[-1,1]} e^{-i\xi\phi} \left(\gamma + i\phi\right)^x d\phi$$

what terminates the proof of the lemma. □

From the exact expressions (12) and (15) of $\mathsf{K}^{-1}(\mathbf{b}_y^{(x)}, \mathbf{w})$, one can easily check that the entries are uniformly bounded in $y$ and $t$ for a given value of $x$, leading to the following lemma:

**Lemma 2.** $\forall x \in \mathbb{Z} \quad \exists M_x > 0 \quad \forall t < t_0 \quad \forall y \in \mathbb{R} \quad \left|\mathsf{K}_{\gamma,t}^{-1}(\mathbf{b}_{x,y}, \mathbf{w})\right| \leq M_x.$

These two lemmas will now be used to prove theorem 1, stating that this family converges weakly to the determinantal random point field on $\mathbb{Z} \times \mathbb{R}$ with kernel $J_\gamma$.

**Theorem 2.** *For each value of $\gamma \in (-1,1)$, the discrete bead model converges weakly when $t$ goes to 0 to a determinantal random point field on $\mathbb{Z} \times \mathbb{R}$. The kernel of this limiting determinant random point field is $J_\gamma$:*

$$J_\gamma(x,\xi) = \begin{cases} \displaystyle\int_{[-1,1]} e^{-i\xi\phi} \left(\gamma + i\phi\sqrt{1-\gamma^2}\right)^x \frac{d\phi}{2\pi} & \text{if } x \geq 0 \\ \displaystyle-\int_{\mathbb{R}\setminus[-1,1]} e^{-i\xi\phi} \left(\gamma + i\phi\sqrt{1-\gamma^2}\right)^x \frac{d\phi}{2\pi} & \text{if } x < 0. \end{cases} \tag{16}$$

*The marginal of the process on a given line is a determinantal random point field on $\mathbb{R}$ with kernel*

$$J_\gamma(0, \xi - \xi') = \frac{\sin(\xi - \xi')}{\pi(\xi - \xi')}. \tag{17}$$

*It is thus the sine random point field of the eigenvalues of large random Hermitian matrices.*

8

*Proof.* Since tightness is automatic for random point fields [4], it is sufficient to prove the convergence of finite dimensional distributions in order to prove the weak convergence of the family of random point fields $(\Omega, \mathcal{F}, \mathbb{P}_{\gamma,\mathtt{t}})$.

Let $I_1, \ldots, I_k$ be segments on wire $x_1, \ldots, x_k$ respectively. It will be convenient to use multi-index notations

$$n! = \prod_{j=1}^{k} n_j!, \quad |n| = \sum_{j=1}^{k} n_j, \quad I^n = I_1^{n_1} \times \cdots \times I_k^{n_k}, \quad z^n = z_1^{n_1} \cdots z_k^{n_k}$$

We will prove the convergence of the moment generating function $G_{\gamma,\mathtt{t}}^{(I)}(z_1, \ldots, z_k)$ of the joint law of $(X_{I_1}, \ldots, X_{I_k})$

$$G_{\gamma,\mathtt{t}}^{(I)}(z) = \mathbb{E}_{\gamma,\mathtt{t}} \left[ \prod_{j=1}^{k} (1 - z_j)^{X_{I_j}} \right] = \sum_{n \in \mathbb{N}^k} \mathbb{E}_{\gamma,\mathtt{t}} \left[ \prod_{j=1}^{k} \frac{(X_{I_j})!}{(X_{I_j} - n_j)!} \right] \frac{(-z)^n}{n!}, \tag{18}$$

where $\mathbb{E}_{\gamma,\mathtt{t}}$ is the expectation with respect to the probability $\mathbb{P}_{\gamma,\mathtt{t}}$ on discrete bead configurations. The factorial moments

$$A_{\gamma,\mathtt{t}}^{(I)}(n_1, \ldots, n_k) = \mathbb{E}_{\gamma,\mathtt{t}} \left[ \prod_{i=1}^{k} \frac{X_{I_i}!}{(X_{I_i} - n_i)!} \right] \tag{19}$$

are quite easy to compute. They are given by the formula:

$$A_{\gamma,\mathtt{t}}^{(I)}(n_1, \ldots, n_k) = \sum_{\substack{y_1^1 \ldots y_{n_1}^1 \in \frac{I_1}{\mathtt{t}\sqrt{1-\gamma^2}} \text{ distinct} \\ y_1^k \ldots y_{n_k}^k \in \frac{I_k}{\mathtt{t}\sqrt{1-\gamma^2}} \text{ distinct}}} \mathbb{P}_{\gamma,\mathtt{t}} \left[ \text{there are beads at } (x_1, \mathtt{t}y_1^1), \ldots, (x_k, \mathtt{t}y_{n_k}^k) \right] \tag{20}$$

where the sum is performed over all the distinct $n_j$tuples of $I_j$, $j = 1, \ldots, k$. By equation (4), this can be rewritten in terms of determinants of matrices with blocks of size $n_1, \ldots, n_k$

$$A_{\gamma,\mathtt{t}}^{(I)}(n) = \sum_{\substack{y_1^1 \ldots y_{n_1}^1 \in \frac{I_1}{\mathtt{t}\sqrt{1-\gamma^2}} \text{ distinct} \\ y_1^k \ldots y_{n_k}^k \in \frac{I_k}{\mathtt{t}\sqrt{1-\gamma^2}} \text{ distinct}}} \mathtt{t}^{|n|} \det \begin{bmatrix} \mathsf{K}_{\gamma,\mathtt{t}}^{-1}(\mathbf{b}_{x_1,y_{i1}}, \mathbf{w}_{x_1,y_{j1}}) & \cdots & \mathsf{K}_{\gamma,\mathtt{t}}^{-1}(\mathbf{b}_{x_k,y_{ik}}, \mathbf{w}_{x_1,y_{j1}}) \\ \vdots & \ddots & \vdots \\ \mathsf{K}_{\gamma,\mathtt{t}}^{-1}(\mathbf{b}_{x_1,y_{i1}}, \mathbf{w}_{x_k,y_{jk}}) & \cdots & \mathsf{K}_{\gamma,\mathtt{t}}^{-1}(\mathbf{b}_{x_k,y_{ik}}, \mathbf{w}_{x_k,y_{jk}}) \end{bmatrix}_{\substack{1 \leq i_1, j_1 \leq n_1 \\ 1 \leq i_k, j_k \leq n_k}} . \tag{21}$$

The determinant in the sum is the same as the one obtained by multiplying which converges when $\mathtt{t}$ goes to zero to

$$A_{\gamma}^{(I)}(n) = \int_{I^n} \det \begin{bmatrix} J_{\gamma}(x_1 - x_1, \xi_{i_1}^{(1)} - \xi_{j_1}^{(1)}) & \cdots & J_{\gamma}(x_1 - x_k, \xi_{i_1}^{(1)} - \xi_{j_k}^{(k)}) \\ \vdots & \ddots & \vdots \\ J_{\gamma}(x_k - x_1, \xi_{i_k}^{(k)} - \xi_{j_1}^{(1)}) & \cdots & J_{\gamma}(x_k - x_k, \xi_{i_k}^{(k)} - \xi_{j_k}^{(k)}) \end{bmatrix} \mathrm{d}^n \xi \tag{22}$$

where the integration variable $\xi$ is the $n$-tuple $\left( \xi_1^{(1)}, \ldots, \xi_{n_1}^{(1)}, \ldots, \xi_{n_k}^{(k)} \right)$. Since the coefficients of $\mathsf{K}_{\gamma,\mathtt{t}}^{-1}$ are bounded uniformly in $\mathtt{t}$ and $y$, say by $M$, then using Hadamard inequality, we get a uniform bound on the coefficients $A_{\gamma,\mathtt{t}}^{(I)}(n_1, \cdots, n_k)$

$$\left| A_{\gamma,\mathtt{t}}^{(I)}(n) \right| \leq \prod_{j=1}^{k} |I_j|^{n_j} \left( \sqrt{|n|} M \right)^{|n|} \tag{23}$$

9

Therefore, by an argument of dominated convergence, the entire series $Q_{\gamma,\mathtt{t}}^{(I)}(z), z \in \mathbb{C}^k$ converges uniformly on compact sets towards

$$Q_\gamma^{(I)}(z) = \sum_{n \in \mathbb{N}^k} A_\gamma^{(I)}(n) \frac{(-z)^n}{n!} \tag{24}$$

which is the moment generating function for the limit distribution of $(X_{I_1}, \ldots, X_{I_k})$. The probability of having for all $j \in \{1, \ldots, k\}$ exactly $n_j$ beads in $I_j$ is given by the following formula

$$\mathbb{P}_\gamma \left[ X_{I_1} = n_1, \ldots, X_{I_k} = n_k \right] = \frac{(-1)^{|n|}}{n!} \frac{\partial^n}{\partial z^n} Q_\gamma^{(I)}(z) \big|_{z=(1,\ldots,1)}. \tag{25}$$

In particular, the probability of having no bead in a Borel set $B$ is given by the Fredholm determinant

$$\mathbb{P}_\gamma \left[ X_B = 0 \right] = \mathrm{Det}(\mathrm{Id} - \chi_B \mathsf{K}_\gamma^{-1} \chi_B) = Q_\gamma^B(1) = \sum_{n=0}^\infty \frac{(-1)^n}{n!} \int_{B^n} \det \left[ J_\gamma(\xi_i - \xi_j) \right] \mathrm{d}^n \xi. \tag{26}$$

$\square$

Many quantities about the continuous bead model can be easily computed, using the underlying dimer model. An example of such a quantity is the average ratio between the distance between a bead and its neighbor on the left and above it, and the distance between two successive beads on the same thread. This average ratio is just the limit of the proportion of $c$-edges among the non horizontal edges in the random dimer configuration of $H$. It is then equal to

$$\mathbb{E}_\gamma \left[ r \right] = \lim_{\mathtt{t} \to 0} \frac{\mathbb{P}_{\gamma,\mathtt{t}} \left[ c\text{-edge} \right]}{\mathbb{P}_{\gamma,\mathtt{t}} \left[ c\text{- or } b\text{-edge} \right]} = \lim_{\mathtt{t} \to 0} \frac{e^{\gamma \mathtt{t}} \mathsf{K}_{\gamma,\mathtt{t}}^{-1}(-1,-1)}{\mathsf{K}_{\gamma,\mathtt{t}}^{-1}(-1,0) + e^{\gamma \mathtt{t}} \mathsf{K}_{\gamma,\mathtt{t}}^{-1}(-1,-1)} = \frac{\arccos \gamma}{\pi}. \tag{27}$$

This quantity would have been difficult to obtain directly from the description of the Gibbs measure for the point process, but has a simple interpretation in terms of dimers.

# 4 Comments and interpretations of the bead model

## 4.1 GUE matrices and uniformly distributed intertwined points

Afterwards, it may seem not so surprising that these configurations of "uniformly" intertwined points are related to the determinantal sine process and more generally to random matrices from the GUE ensemble.

Take a random (finite) matrix $H_n$ from the GUE ensemble, and define for $k \in \{1, \ldots, n\}$, $H_n^{(k)} = (H_n)_{1 \le i,j \le k}$ to be the submatrix of $H_n$ formed by the first $k$ rows and $k$ columns of $H_n$. Let $\lambda_1^{(k)} \le \lambda_k^{(k)}$ be the eigenvalues of $H_n^{(k)}$. It follows directly from the mini-max formulation for the eigenvalues that

$$\forall \, k \in \{1, \ldots, n\}, \, \forall \, j \in \{1, \ldots k\} \quad \lambda_j^{(k+1)} \le \lambda_j^{(k)} \le \lambda_{j+1}^{(k+1)}. \tag{28}$$

Moreover, a result of Baryshnikov [2] states that if we condition on the eigenvalues $\lambda_1, \ldots, \lambda_n$ of $H_n$, then the eigenvalues of the submatrices are uniformly distributed in the simplex

$$\mathcal{S}_{(\lambda_1,\ldots,\lambda_n)} = \left\{ (x_j^{(k)})_{\substack{1 \le k \le n-1 \\ 1 \le j \le k}} \, | \lambda_j \le x_j^{(n-1)} \le \lambda_{j+1} \, ; \, x_j^{(k+1)} \le x_j^{(k)} \le x_{j+1}^{(k+1)} \right\}. \tag{29}$$

The bead model is somehow a bi-infinite analogue of this.

## 4.2   The bead model as an asymmetric exclusion process

A bead configuration can be interpreted as the history of a collection of particles located on a one dimensional lattice $\mathbb{Z}$ and jumping from left to right. Time is continuous and is flowing vertically along the threads, and there is a lattice site between two successive threads. Joining every bead to the bead just above it on the neighboring right thread, one gets an infinite collection of monotonous paths representing the trajectories of the particles: a bead on a thread corresponds to a jump of a particle from the site at the left of the thread to the site on its right. Because of the geometric constraint on beads, these paths cannot touch each other. Consequently, the particles are submitted to an exclusion rule: a particle cannot jump to a site if this one is already occupied by another particle.
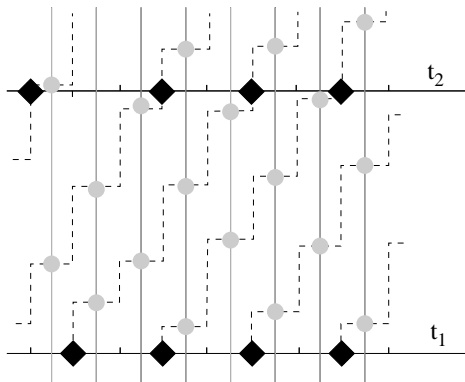


Figure 4: The trajectories corresponding to the bead configuration of figure 1 and positions of particles (black squares) at different times $t_1$ and $t_2$.

The Gibbs measures $\mathbb{P}_\gamma$ on bead configurations, viewed as families of monotonous paths constructed as above, are probability measures on all possible evolutions of particles. The Gibbs property and ergodicity imply that the marginal of these measures for a fixed time ( *i.e.* along an horizontal line) give stationary measures for some Markovian dynamics.

The discrete bead model gives a discrete version of this particle system: in this picture a particle is represented by a $c$-edge, and a hole by a $b$-edge. Under $\mathbb{P}_\gamma$, the average particle density $\rho$ is equal to the limit of the probability of a $c$-edge, and therefore related to $\gamma$ by the following expression

$$\rho = \lim_{\mathtt{t} \to 0} \mathbb{P}_{\mathtt{t},\gamma}\left[c\text{-edge}\right] = 1 - \frac{\arccos \gamma}{\pi} \tag{30}$$

so that the density is an increasing function of $\gamma$.

The Asymmetric Simple Exclusion Process (ASEP) is also an example of particle systems with the same constraint of exclusion. Its evolution is Markovian, and the transition rates from an allowed configuration to another is constant. The translation invariant stationary measures for this model are Bernoulli probability measure, whose parameter is the density.

If the particles are not located on the vertices of the finite lattice $\mathbb{Z}$ but on a finite annulus $\mathbb{Z}/N\mathbb{Z}$, then the number of particles is a conserved quantity. For a fixed number of particles, the

stationary measure is uniform for ASEP. This is not the case for the bead model with a finite number of beads[1] the probability of a configuration of particles depends not only on the number of particles, but also on their positions.

The properties of the particle system coming from the bead model differ from that of ASEP. It would be interesting to study more in details these properties using the dimer microscopic structure, and to compare them with that of ASEP, that are also related to random matrix theory [14].

# 5 The bead model as a universal limit for dimer models

Although the bead model was presented in the last section as the limit of the dimer model on the honeycomb lattice, it turns out to be much more general. Indeed, the bead model appears as the limit of any dimer model on a planar $\mathbb{Z}^2$-periodic bipartite graph. We first recall some facts from the theory of the dimer model on a planar bipartite lattice(see [9, 8] for more details).

## 5.1 The dimer model on a bipartite planar periodic graph

Let $G$ be a planar bipartite $\mathbb{Z}^2$-periodic graph, together with a periodic weight function on the edges of $G$. We suppose that the fundamental domain, delimited by an horizontal path $\gamma_x$ and a vertical path $\gamma_y$, contains $n$ black vertices $\mathbf{b}_1, \ldots, \mathbf{b}_n$ and $n$ white vertices $\mathbf{w}_1, \ldots, \mathbf{w}_n$, and that $G$ has at least one dimer configuration.

There is a two-parameter family of Gibbs measures on dimer configurations of $G$ for these weights, parameterized by the two component of an external magnetic field $(B_x, B_y)$ [9]. One can associate to this weighted graph, as in the case of the honeycomb lattice, a *Kasteleyn operator* $\mathsf{K}$ that will describe the dimer model on $G$. For a given value of the magnetic field $B$, the probability that some edges $\mathbf{e}_1 = (\mathbf{w}_1, \mathbf{b}_1), \ldots, \mathbf{e}_k = (\mathbf{w}_k, \mathbf{b}_k)$ appear in the random dimer configuration is given by the following formula

$$\mathbb{P}_B\left[\mathbf{e}_1, \ldots, \mathbf{e}_k\right] = \left(\prod_{j=1}^k \mathsf{K}(\mathbf{w}_j, \mathbf{b}_j)\right) \det_{1 \leq i,j \leq k}\left[\mathsf{K}_B^{-1}(\mathbf{b}_i, \mathbf{w}_j)\right] \tag{31}$$

where the entries of $\mathsf{K}_B^{-1}$ are given by the inverse Fourier transform

$$\mathsf{K}_B^{-1}(\mathbf{b}_{x,y}^j, \mathbf{w}^i) = \iint_{\mathbb{T}^2} \left[K(e^{B_x}z, e^{B_y}w)\right]_{j,i}^{-1} \frac{\mathrm{d}z}{2i\pi z}\frac{\mathrm{d}w}{2i\pi w} = \iint_{\mathbb{T}^2} \frac{Q_{j,i}(e^{B_x}z, e^{B_y}w)}{P(e^{B_x}z, e^{B_y}w)} \frac{\mathrm{d}z}{2i\pi z}\frac{\mathrm{d}w}{2i\pi w} \tag{32}$$

The *characteristic polynomial* $P(z, w)$ is the determinant of the Fourier transform $K(z, w)$ of the periodic operator $\mathsf{K}$, and $Q(z, w)$ is the comatrix of $K(z, w)$. The asymptotics of $\mathsf{K}_B^{-1}$ and thus the correlations decay depend on the regularity of the integrand in (32), and in particular on the presence of zeros of $P(e^{B_x}z, e^{B_y}w)$ on the unit torus.

The *spectral curve* $\{(z, w) \in \mathbb{C}^2 \mid P(z, w) = 0\}$ is a complex algebraic curve of a special kind : it is a *Harnack curve* [8, 13, 12]. For generic values of $(B_x, B_y)$, $P(e^{B_x}z, e^{B_y}w)$ has zero or two roots

---

[1]A bead model for a finite number of threads can be constructed following the same procedure as in the beginning of this article. We impose the number of threads $N$ to be even to ensure that the geometric constraint on beads makes sense. We get leading to a 1-parameter family of determinantal random fields, whose kernel is obtained by replacing the integral in (7) by a discrete sum.

on the unit torus, and the phase diagram describing the behavior of the measures in function of $B_x$ and $B_y$ is given by the *amœba* of the *spectral curve*, *i.e.* the image of $P(z, w) = 0$ by the mapping

$$\text{Log} : (\mathbb{C}^*)^2 \to \mathbb{R}^2$$
$$(z, w) \mapsto (\log|z|, \log|w|).$$

When $(B_x, B_y)$ lies in the interior of the amœba, the characteristic polynomial $P(e^{B_x}z, e^{B_y}w)$ has two conjugate roots on the unit torus and the correlations decay polynomially, and the corresponding measure is said to be *liquid*. When $(B_x, B_y)$ lies inside a bounded connected component of the amœba, the correlations decay exponentially fast, and the measure is *gaseous*. When $(B_x, B_y)$ lies in a unbounded complementary component of the amœba, the measure is said to be *solid* and there are infinite deterministic dual paths crossing no dimers with probability 1.

The existence of a dimer configuration on $G$ is equivalent to that of a dimer configuration on the torus $G_1 = G/\mathbb{Z}^2$. We suppose that such a configuration on $G_1$ exists, that can be lifted to a periodic dimer configuration $\mathcal{C}_0$ of $G$. A dimer configuration $\mathcal{C}$ can be interpreted as *white-to-black unit flow*, *i.e.* a 1-form with divergence +1 at each white vertex, and divergence -1 at each black vertex. Therefore, the difference $\mathcal{C} - \mathcal{C}_0$ is a divergence-free flow. The horizontal (resp. vertical) *slope* of a Gibbs measure $\mu$ is the expected amount for $\mu$ of the flow $\mathcal{C} - \mathcal{C}_0$ across $-\gamma_y$ (resp. $\gamma_x$). Two Gibbs measures having the same slope are in fact equal [15, 9]. The *Newton polygon* $N(P)$ of $P$, the convex hull of the exponents of monomials of $P$, coincide with the set of all possible slopes for a Gibbs measure on dimer configurations. The structure of this amœba is related to the geometry of $N(P)$ through the *Ronkine function* [11]

$$R : (B_x, B_y) \mapsto \iint_{\mathbb{T}^2} \log\big(P(e^{B_x}z, e^{B_y}w)\big) \frac{\mathrm{d}z}{2i\pi z} \frac{\mathrm{d}w}{2i\pi w}. \tag{33}$$

In particular, the solid and gaseous phases are mapped to integer points of $N(P)$.

To clarify all these notions, we apply them to the particular example of the honeycomb lattice we discussed before: choosing weights $a$, $b$, $c$ for edges according to their orientation (without magnetic field) is in fact equivalent to choosing all weights equal to $a = \mathtt{t}$ and imposing a magnetic field equal to $B_x = \log(c/b) = \gamma\mathtt{t}$, $B_y = \log(a/b) = \log\mathtt{t}$. The fundamental domain of the honeycomb lattice is constituted by one black vertex and one white vertex. Therefore, the Fourier transform $K(z, w)$ is $1 \times 1$ matrix:$K(z, w) = \mathtt{t}(1 + 1/w + z/w)$. The characteristic polynomial $P(z, w)$ is therefore also equal to $\mathtt{t}(1 + 1/w + z/w)$, such that

$$P(e^{B_x}z, e^{B_y}w) = \mathtt{t} + \frac{1}{w}(1 + ze^{\gamma\mathtt{t}}). \tag{34}$$

The cofactor $Q(z, w)$ of $K(z, w)$ is by convention equal to 1. The Newton polygon and the amœba for this model are represented on figure 5.

The bead model is obtained from the dimer model on the honeycomb lattice when the magnetic field goes inside one of the outgrowths of the amœba, in the thin region separating two solid phases. In the general dimer model, the bead model will also appear near the frontier between the liquid phase and solid phases. But before explaining how to find the bead model in this setting, we need some more information about the local geometry of the amœba, in particular about its unbounded outgrowths of the amœba: the *tentacles*.
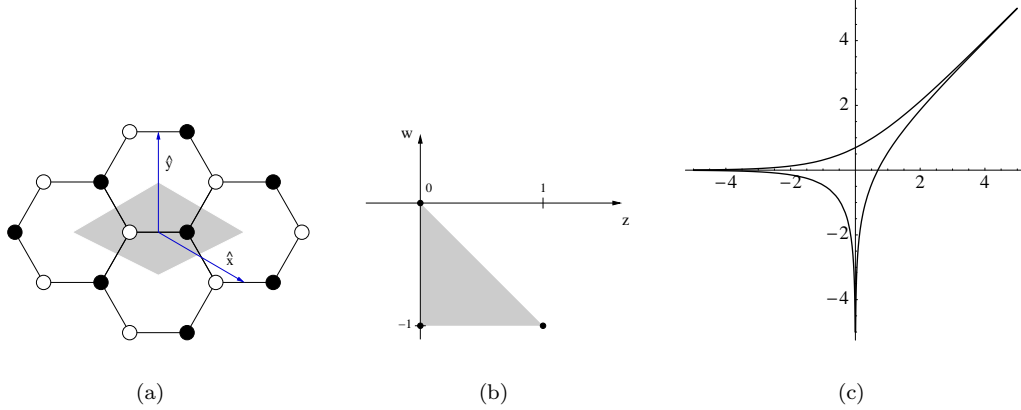
Figure 5: The dimer model on the honeycomb lattice: (a) the fundamental domain of the graph, (b) the Newton polygon $N(P)$ of the characteristic polynomial $P(z, w) = 1 + (1 + z)/w$, and (c) the amœba of $P$ in the plane $(B_x, B_y)$.

## 5.2 Tentacles of the amoeba

Consider a particular side of the Newton polygon $N(P)$. Changing the generators of the $\mathbb{Z}^2$ lattice acting on $G$ by translation induces a linear transformation of $N(P)$. A change of basis of $\mathbb{Z}^2$ is encoded by an element $M$ of $\mathrm{SL}_2(\mathbb{Z})$. The linear transformation acting on $N(P)$ is $(M^{-1})^T$. After possibly such an operation, we can assume that this side is horizontal, and that the polygon lies above it. Recall that the Newton polygon represents the possible slopes for a Gibbs measure on the dimer model on $G$. When the slope of a Gibbs measure is a lattice point of the boundary of $N(P)$, the system is a solid phase.

We want to investigate the geometry of the phase diagram for values of the magnetic field inducing measures with a slope close to the particular side of $N(P)$ we chose. In particular, we seek for the shape of the curve in the neighborhood of the frontier between the liquid phase and the different solid phases, corresponding to the points of the particular side of the polygon.

To get a measure with a slope close to that side of $N(P)$, we apply to the system a magnetic field oriented essentially downward $(B_x, B_y) = (c, -R)$. To remain close to the notations used in the previous section, we introduce the small parameter $\mathtt{t} = e^{-R}$.

When $\mathtt{t}$ is small, the leading terms in the characteristic polynomial $P(e^c z, \mathtt{t}w)$ are those with the smallest power in $w$, say $\delta_0$.

$$P(e^c z, \mathtt{t}w) = (\mathtt{t}w)^{\delta_0} \Big( \sum_{\gamma} a_{\gamma \delta_0} (e^c z)^{\gamma} + O(\mathtt{t}) \Big) \tag{35}$$

By a suitable choice of the origin of the Newton polygon (deforming the paths $\gamma_x$ and/or $\gamma_y$ delimiting the fundamental domain of $G$), one can assume that $\delta_0 = 0$ and that all the roots of $P_0(X) = \sum_{\gamma} a_{\gamma 0} X^{\gamma}$ are positive [9].

If $e^c$ is not a root of $P_0(X) = \sum_{\gamma} a_{\gamma 0} X^{\gamma}$, then for $\mathtt{t}$ small enough, $P(e^c z, e^{-R} w)$ has no roots on the unit torus. In this case, the magnetic field $(B_x, B_y) = (c, -R)$ belongs to a unbounded component of the amœba. The corresponding measure $\mu(B_x, B_y)$ is frozen. On the contrary, if

14

$e^c$ is a root of this polynomial, then for every $R$ large enough, the polynomial has two complex conjugated roots on the unit torus: we are in the liquid phase. The amœba defining the liquid phase has therefore *tentacles* going to infinity with asymptotes given by the straight lines $x = c$.

For generic weights, the asymptotes are all distinct, and there is one asymptote for each segment between to lattice points on the side of $N(P)$. Moreover, one can give an asymptotic expansion for the equation of the boundary of the amœba: since the boundary of the amœba is the image of the real locus of the curve, it is given by the equation

$$P(\pm e^{B_x}, \pm e^{B_y}) = 0 \tag{36}$$

In the neighborhood of $(B_x, B_y) = (c, -\infty)$, $B_x$ admits an asymptotic expansion in $\mathtt{t} = e^{-B_y}$: $B_x = c + c_1\mathtt{t} + O(\mathtt{t}^2)$. Since $P(e^c, 0) = 0$, we have

$$P(e^{B_x}, \pm e^{B_y}) = P(e^{c+c_1\mathtt{t}+O(\mathtt{t}^2)}, \pm\mathtt{t}) = \left(c_1 e^c \partial_1 P(e^c, 0) \pm \partial_2 P(e^c, 0)\right)\mathtt{t} + O(\mathtt{t}^2) \tag{37}$$

Therefore the coefficient $c_1$ in the expansion is defined by

$$c_1 = \pm \frac{\partial_2 P(e^c, 0)}{e^c \partial_1 P(e^c, 0)} \tag{38}$$

and the two curves $B_x = c \pm e^{-c}\frac{\partial_2 P(e^c,0)}{\partial_1 P(e^c,0)}e^{B_y}$ define asymptotic branches of the boundary of the amœba in the neighborhood of $(c, -\infty)$. Define $\beta$ as

$$\beta = -e^{-c}\frac{\partial_2 P(e^c, 0)}{\partial_1 P(e^c, 0)} \tag{39}$$

For any $\gamma \in (-1, 1)$, the curve

$$B_x = c + \gamma \beta e^{B_y} \tag{40}$$

lies inside the amoeba for $B_y$ negative enough.

## 5.3 Deep inside a tentacle

### 5.3.1 Analytic results about the roots of $P$

Let us fix $c$ to be equal, as before, to the logarithm of one of the roots of $P_0$. For a fixed $z$, the polynomial $P(e^{c+\gamma\beta\mathtt{t}}z, W)$ has $d$ roots $W_0(z), \ldots, W_{d-1}(z)$. Since $e^c$ is a root of $P_0$, one of these $W_j(z)$, say it is $W_0$, equals $0$ when $z = 1$. If all the roots of $P_0$ are distinct, $W_0(z)$ is the only zero having this property. The 2-to-1 property shows that $W_0(z)$ does not equal zero for $z \neq 1$

Therefore, by compactness of $\mathbb{S}^1$ there exists an $\epsilon > 0$ such that

$$\forall\, j \in \{1, \ldots, d-1\}, \ \ \forall\, z \in \mathbb{S}^1 \ \ |W_j(z)| \geq \epsilon \tag{41}$$

Differentiability of the roots with respect to the coefficients and symmetry by complex conjugation imply that there exists $\theta(\mathtt{t}) = \theta_0\mathtt{t} + O(\mathtt{t}^2)$, with $\theta_0 > 0$ such that

$$|W_0(z)| \leq \mathtt{t} \ \Leftrightarrow \ z \in [e^{-i\theta(\mathtt{t})}, e^{i\theta(\mathtt{t})}] \tag{42}$$

In fact, an expansion of $P$ similar to (37) shows that when $\arg(z) = O(\mathtt{t})$

$$W_0(z) = \gamma\mathtt{t} + \frac{i\arg(z)}{\beta} + O(\mathtt{t}^2), \tag{43}$$

and therefore, $\theta(\mathtt{t}) = \mathtt{t}\beta\sqrt{1 - \gamma^2} + O(\mathtt{t}^2)$.
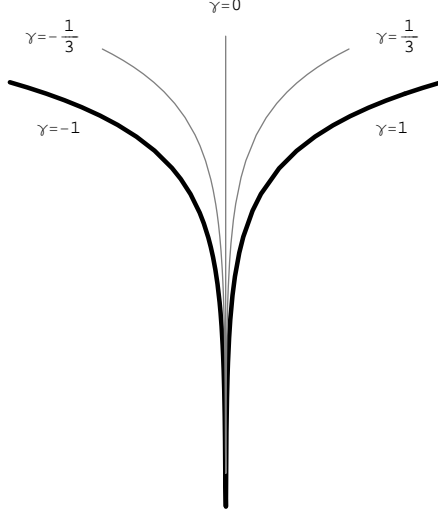
15

Figure 6: A tentacle (in thick lines) and curves described above, for different values of $\gamma$.

### 5.3.2 Asymptotics of the inverse Kasteleyn operator inside a tentacle

The Newton polygon $N(P)$ can also be obtained indirectly from the *max flow-min cut* theorem as the intersections of half-planes made of points satisfying linear constraints to be a slope of measure on dimer coverings [9].

The side of the Newton polygon we are looking at is a segment of one of the straight lines delimiting one of these half-planes. When the average slope of the Gibbs measure lies on this line, one of the inequalities defining $N(P)$ becomes an equality, implying the existence of *frozen dual paths*, with a direction perpendicular to the side of $N(P)$, that are not crossed by any dimer with probability 1. These possibly frozen paths will be the threads of our bead model. When the slope is not exactly on that boundary of $N(P)$, some dimers may cross these paths. We will see that these *defects* will play the role of beads strung along these threads.

Let $\mathbf{e} = (\mathbf{w}, \mathbf{b})$ be an edge of $G$ crossing one of these threads. When the slope of the Gibbs measure is on the side of the Newton polygon, this edge appears in the random dimer configuration with probability 0. In particular, there is no dimer configuration on the torus $G_1 = G/\mathbb{Z}^2$ corresponding to a lattice point of the side of $N(P)$ containing this edge. As the cofactor $Q_{\mathbf{e}}(z, w) = Q_{\mathbf{bw}}(z, w)$ is up to a sign the determinant of the Kasteleyn operator on $G_1 \setminus \{\mathbf{w}, \mathbf{b}\}$, it contains only monomials of degree at least 1 in $w$ (otherwise, there would have been a Gibbs measure with a slope on the side of $N(P)$ for which $\mathbf{e}$ is a dimer with positive probability, what is in contradiction with the fact that $\mathbf{e}$ crosses a frozen path).

We determine now the asymptotic expression for the coupling function $\mathsf{K}_{\gamma,\mathbf{t}}^{-1}(\mathbf{b_x}, \mathbf{w})$ corresponding to our magnetic field $(B_x, B_y) = (c + \beta\gamma\mathbf{t}, \log\mathbf{t})$, between $\mathbf{w}$ and the black end $\mathbf{b_x}$ of a translate $\mathbf{e_x}$ of $\mathbf{e}$ by $\mathbf{x} = (x, y) \in \mathbb{Z}^2$

$$\mathsf{K}_{\gamma,\mathbf{t}}^{-1}(\mathbf{b_x}, \mathbf{w}) = \iint \frac{z^{-y} w^x Q_{\mathbf{e}}(e^{c+\beta\gamma\mathbf{t}}z, \mathbf{t}w)}{P(e^{c+\beta\gamma\mathbf{t}}z, \mathbf{t}w)} \frac{\mathrm{d}z}{2i\pi z} \frac{\mathrm{d}w}{2i\pi w}. \tag{44}$$

16

**Proposition 1.** *Denote by $J_\gamma(x, \xi)$ the kernel of the bead model.*

$$J_\gamma(x, \xi) = \begin{cases} \displaystyle\int\!\!\!\!\int_{[-1,1]} e^{-i\xi\phi}(\gamma + i\phi\sqrt{1-\gamma^2})^x \frac{d\phi}{2\pi} & \text{if } x \geq 0 \\ \displaystyle-\int_{\mathbb{R}\setminus[-1,1]} e^{-i\xi\phi}(\gamma + i\phi\sqrt{1-\gamma^2})^x \frac{d\phi}{2\pi} & \text{if } x < 0 \end{cases} \tag{45}$$

*In the scaling limit $\mathsf{t} \to 0$, , $\mathsf{t}\beta y\sqrt{1-\gamma^2} \to \xi$, the coefficients $\mathsf{K}_{\gamma,\mathsf{t}}^{-1}(\mathbf{b_x}, \mathbf{w})$ have the following asymptotics*

$$\mathsf{K}_{\gamma,\mathsf{t}}^{-1}(\mathbf{b_x}, \mathbf{w}) \sim \mathsf{t}\rho_{\mathbf{e}}\sqrt{1-\gamma^2}J_\alpha(x, \xi), \tag{46}$$

*where the quantity $\rho_{\mathbf{e}}$ is given by*

$$\rho_{\mathbf{e}} = \frac{\partial_2 Q_{\mathbf{e}}(e^c, 0)}{\partial_2 P(e^c, 0)}. \tag{47}$$

*Once multiplied by $K_{\mathbf{e}}$, it represents the proportion of this type of edges among the defects along a thread.*

*Proof.* We denote by $f(z, w)$ the rational fraction inside the integral (44)

$$f(z, w) = \frac{z^{-y-1}w^{x-1}Q_{\mathbf{e}}(e^{c+\beta\gamma\mathsf{t}}z, \mathsf{t}w)}{P(e^{c+\beta\gamma\mathsf{t}}z, \mathsf{t}w)}. \tag{48}$$

The integral defining $\mathsf{K}_{\gamma,\mathsf{t}}^{-1}$ is evaluated by performing first the integral over $w$. Suppose first that $x \geq 0$. There is no singularity at $w = 0$, since $\deg_w Q \geq 1$. The only pole in the unit disc is $W_0(z)/\mathsf{t}$ when $z \in \left[e^{-i\theta(\mathsf{t})}, e^{i\theta(\mathsf{t})}\right] = I_\mathsf{t}$. In this case, we introduce $\zeta(\phi) = \gamma + i\phi\sqrt{1-\gamma^2}$ with $z = e^{i\beta\mathsf{t}\phi\sqrt{1-\gamma^2}}$, and get:

$$\mathsf{K}_{\gamma,\mathsf{t}}^{-1}(\mathbf{b_x}, \mathbf{w}) = \int_{I_\mathsf{t}} \frac{z^{-y}\left(W_0(z)/\mathsf{t}\right)^{x-1}Q_{\mathbf{e}}(e^{c+\beta\gamma\mathsf{t}}z, W_0(z))}{\partial_2 P(z, W_0(z))\mathsf{t}} \frac{dz}{2i\pi z}$$

$$= \sqrt{1-\gamma^2}\int_{-1+O(\mathsf{t})}^{1+O(\mathsf{t})} \frac{e^{-i\beta\mathsf{t}y\phi\sqrt{1-\gamma^2}}(\zeta(\phi) + O(\mathsf{t}))^{x-1}\, Q_{\mathbf{e}}(e^{c+\mathsf{t}\beta\zeta(\phi)}, \mathsf{t}\zeta(\phi) + O(\mathsf{t}^2))}{\partial_2 P(e^{c+\mathsf{t}\beta\zeta(\phi)}, \mathsf{t}\zeta(\phi) + O(\mathsf{t}^2))} \frac{\beta d\phi}{2\pi}. \tag{49}$$

For a small $\mathsf{t}$ and a fixed $\phi$, we have

$$Q_{\mathbf{e}}(e^{c+\mathsf{t}\beta\zeta(\phi)}, \mathsf{t}\zeta(\phi) + O(\mathsf{t}^2)) = \mathsf{t}\zeta(\phi)\partial_2 Q_{\mathbf{e}} + O(\mathsf{t}^2), \tag{50}$$

$$\partial_2 P(e^{c+\mathsf{t}\beta\zeta(\phi)}, \mathsf{t}\zeta(\phi) + O(\mathsf{t}^2)) = \partial_2 P + O(\mathsf{t}). \tag{51}$$

where the derivatives of polynomials $P$ and $Q_{\mathbf{e}}$ without specified point are evaluated at $(e^c, 0)$. For the first expansion, we used the fact that $Q_{\mathbf{e}}(z, 0) \equiv 0$ and therefore $\partial_1 Q_{\mathbf{e}} = 0$. Therefore,

$$\mathsf{K}_{\gamma,\mathsf{t}}^{-1}(\mathbf{b_x}, \mathbf{w}) = \mathsf{t}\beta\sqrt{1-\gamma^2}\frac{\partial_2 Q_{\mathbf{e}}}{\partial_2 P}\left(\int_{[-1,1]} e^{-i\xi\phi}\zeta(\phi)^x \frac{d\phi}{2\pi} + O(\mathsf{t})\right)$$

$$= \mathsf{t}\beta\sqrt{1-\gamma^2}\rho_e\left(\int_{[-1,1]} e^{-i\xi\phi}(\gamma + i\phi\sqrt{1-\gamma^2})^x \frac{d\phi}{2\pi} + O(\mathsf{t})\right)$$

17

When $x < 0$, the rational fraction in the integral has a multiple pole at $w = 0$ which is hard to evaluate directly. However the rational fraction is a $o(\frac{1}{w})$ when $|w| \to \infty$, and hence the sum of all residues in the plane is 0.

Let us bound the residues at the simple roots of $P$: $W_1(z), \ldots, W_{d-1}(z)$. We know already from (41) that there exists $\epsilon$ such that for every $j \in \{1, \ldots, d-1\}$, $|W_j(z)| \geq \epsilon$ for every $z \in \mathbb{S}^1$. By the same argument of compactness, there exists a constant $M > 0$ such that for $\mathtt{t}$ small enough,

$$\forall \, j \in \{1, \ldots, d-1\} \ \ \forall \, z \in \mathbb{S}^1$$

$$\left| \partial_2 P(e^{c+\beta\gamma\mathtt{t}} z, W_j(z)) \right| \geq \frac{1}{M} \quad \text{and} \quad \left| \frac{Q_{\mathbf{e}}(e^{c+\beta\gamma\mathtt{t}} z, W_j(z))}{W_j(z)} \right| \leq M \quad (52)$$

and therefore,

$$\left| \frac{(W_j(z)/\mathtt{t})^x Q_{\mathbf{e}}(e^{c+\gamma\beta\mathtt{t}}, W_j(z))}{W_j(z) \partial_2 P(e^{c+\gamma\beta\mathtt{t}} z, W_j(z))} \right| \leq (\epsilon/\mathtt{t})^x M^2 = O(\mathtt{t}^{-x}) \quad (53)$$

Thus the contribution of these residues is negligible as soon as $x \leq -2$. In that case, we have:

$$\mathsf{K}_{\gamma,\mathtt{t}}^{-1}(\mathbf{b_x}, \mathbf{w}) = \int_{\mathbb{S}^1} \operatorname{Res}_{w=0} f(z, w) \frac{\mathrm{d}z}{2i\pi} + \int_{I_{\mathtt{t}}} \operatorname{Res}_{w=W_0(z)/\mathtt{t}} f(z, w) \frac{\mathrm{d}z}{2i\pi}$$

$$= -\sum_{j=1}^{d-1} \int_{\mathbb{S}^1} \operatorname{Res}_{w=W_j(z)/\mathtt{t}} f(z, w) \frac{\mathrm{d}z}{2i\pi} - \int_{\mathbb{S}^1 \setminus I_{\mathtt{t}}} \operatorname{Res}_{w=W_0(z)/\mathtt{t}} f(z, w) \frac{\mathrm{d}z}{2i\pi} \quad (54)$$

Using the estimates (50) and (51), we find, using the same change of variable $z = e^{i\beta\mathtt{t}\sqrt{1-\gamma^2}\phi}$ as above, that

$$\int_{\mathbb{S}^1 \setminus I_{\mathtt{t}}} \operatorname{Res}_{w=W_0(z)/\mathtt{t}} f(z, w) \frac{\mathrm{d}z}{2i\pi} = \int_{\mathbb{S}^1 \setminus I_{\mathtt{t}}} \frac{z^{-y} \left(\frac{W_0(z)}{\mathtt{t}}\right)^{x-1} Q_{\mathbf{e}}(e^{c+\gamma\beta\mathtt{t}} z, W_0(z))}{\mathtt{t} \partial_2 P(e^{c+\gamma\beta\mathtt{t}} z, W_0(z))} \frac{\mathrm{d}z}{2i\pi z}$$

$$= \mathtt{t}\beta\sqrt{1-\gamma^2} \left( \int_{-\frac{\pi}{|\beta|\mathtt{t}\sqrt{1-\gamma^2}}}^{-1+o(1)} + \int_{1+o(1)}^{\overline{\frac{\pi}{|\beta|\mathtt{t}\sqrt{1-\gamma^2}}}} \right) \frac{e^{-iy\beta\mathtt{t}\phi\sqrt{1-\gamma^2}}(\zeta(\phi) + O(\mathtt{t}))^{x-1}}{\mathtt{t}\partial_2 P(e^{c+\beta\mathtt{t}\zeta(\phi)}, \mathtt{t}\zeta(\phi) + O(\mathtt{t}^2))} \times$$

$$Q_{\mathbf{e}}(e^{c+\mathtt{t}\beta\zeta(\phi)}, \mathtt{t}\zeta(\phi) + O(\mathtt{t}^2)) \frac{\mathrm{d}\phi}{2\pi}. \quad (55)$$

By Lebesgue's dominated convergence theorem, and by 50 and 51, the integral is asymptotic in the scaling limit $\mathtt{t} \to 0$, $\mathtt{t}\beta y \sqrt{1-\gamma^2} \to \xi$ to the following expression

$$\frac{\partial_2 Q_{\mathbf{e}}}{\partial_2 P} \int_{\mathbb{R} \setminus [-1,1]} e^{-i\phi\xi} (\gamma + i\phi\sqrt{1-\gamma^2})^x \frac{\mathrm{d}\phi}{2\pi} \quad (56)$$

and thus,

$$\mathsf{K}_{\gamma,\mathtt{t}}^{-1}(\mathbf{b_x}, \mathbf{w}) = \frac{\mathtt{t}\beta\sqrt{1-\gamma^2}\partial_2 Q_{\mathbf{e}}}{\partial_2 P} \left( -\int_{\mathbb{R} \setminus [-1,1]} e^{-i\phi\xi} (\gamma + i\phi\sqrt{1-\gamma^2})^x \frac{\mathrm{d}\phi}{2\pi} + o(1) \right). \quad (57)$$

18

When $x = -1$, the residues at the poles $W_1(z), \ldots, W_{d-1}(z)$ are not negligible any more. However, in this case, the pole at $w = 0$ is simple. A direct evaluation of the integral shows:

$$
\mathsf{K}^{-1}_{\gamma,\mathsf{t}}(\mathbf{b}_{(-1,y)}, \mathbf{w}) = \int_{\mathbb{S}^1} \mathrm{Res}_{w=0}\, f(z,w) \frac{\mathrm{d}z}{2i\pi} + \int_{I_{\mathsf{t}}} \mathrm{Res}_{w=W_0(z)/\mathsf{t}}\, f(z,w) \frac{\mathrm{d}z}{2i\pi}
$$

$$
= \int_{\mathbb{S}^1} \frac{z^{-y}\mathsf{t}\partial_2 Q_{\mathbf{e}}(e^{c+\beta\gamma\mathsf{t}}z, 0)}{P(e^{c+\beta\gamma\mathsf{t}}z, 0)} \frac{\mathrm{d}z}{2i\pi z} + \int_{I_{\mathsf{t}}} \frac{z^{-y}\left(\frac{W_0(z)}{\mathsf{t}}\right)^{-2} Q_{\mathbf{e}}(e^{c+\beta\gamma\mathsf{t}}z, W_0(z))}{\mathsf{t}\partial_2 P(e^{c+\beta\gamma\mathsf{t}}z, W_0(z))} \frac{\mathrm{d}z}{2i\pi z} \quad (58)
$$

Posing again $z = e^{i\beta\mathsf{t}\phi\sqrt{1-\gamma^2}}$ and $\zeta(\phi) = \gamma + i\phi\sqrt{1-\gamma^2}$, one has

$$
\mathsf{K}^{-1}_{\gamma,\mathsf{t}}(\mathbf{b}_{\mathbf{x}}, \mathbf{w}) = \mathsf{t}^2\beta\sqrt{1-\gamma^2} \int_{-\frac{\pi}{|\beta|\mathsf{t}\sqrt{1-\gamma^2}}}^{\frac{\pi}{|\beta|\mathsf{t}\sqrt{1-\gamma^2}}} \frac{e^{-i\beta\varphi\mathsf{t}y\sqrt{1-\gamma^2}}\partial_2 Q_{\mathbf{e}}(e^{c+\beta\mathsf{t}\zeta(\phi)}, 0)}{P(e^{c+\beta\mathsf{t}\zeta(\phi)}, 0)} \frac{\mathrm{d}\phi}{2\pi}
$$

$$
+ \mathsf{t}^2\beta\sqrt{1-\gamma^2} \int_{-1+o(1)}^{1+o(1)} \frac{e^{-i\beta\varphi\mathsf{t}y\sqrt{1-\gamma^2}} Q_{\mathbf{e}}(e^{c+\beta\mathsf{t}\zeta(\phi)}, 0)}{W_0(e^{i\beta\phi\mathsf{t}\sqrt{1-\gamma^2}})^2 \partial_2 P(e^{c+\beta\mathsf{t}\zeta(\phi)}, 0)} \frac{\mathrm{d}\phi}{2\pi} \quad (59)
$$

Using the following estimates from Taylor's formula

$$
\partial_2 Q(e^{c+\beta\mathsf{t}\zeta(\phi)}, 0) = \partial_2 Q_{\mathbf{e}} + O(\mathsf{t}) \quad (60)
$$

$$
P(e^{c+\beta\mathsf{t}\zeta(\phi)}, 0) = P(e^{c+\beta\gamma\mathsf{t}+i\beta\mathsf{t}\zeta(\phi)}, W_0(z)) - W_0(z)\partial_2 P(e^{c+\beta\mathsf{t}\zeta(\phi)}, W_0(z)) + O(\mathsf{t}^2)
$$

$$
= 0 - \mathsf{t}\zeta(\phi)(\partial_2 P + O(\mathsf{t})) = -\mathsf{t}\zeta(\phi)\partial_2 P + O(\mathsf{t}^2) \quad (61)
$$

together with (50) and (51), and applying Lebesgue dominated convergence theorem after an integration by parts, one can prove that in the scaling limit, the coefficient of the inverse Kasteleyn operator $\mathsf{K}^{-1}_{\gamma,\mathsf{t}}(\mathbf{b}_{\mathbf{x}}, \mathbf{w})$ is asymptotic to

$$
-\mathsf{t}\beta\sqrt{1-\gamma^2}\frac{\partial_2 Q}{\partial_2 P} \int_{\mathbb{R}\setminus[-1,1]} e^{-i\phi\xi}(\gamma + i\phi\sqrt{1-\gamma^2})^{-1}\frac{\mathrm{d}\phi}{2\pi}
$$

$\square$

*Remark.* The ratio $\partial_2 Q_{\mathbf{e}}/\partial_2 P$ controls the density of the limiting bead model. If one plugs the value $\phi = 1$ into (50) and (51), one can see that it is, up to terms of higher order in $\mathsf{t}$, equal to

$$
\frac{iQ_{\mathbf{e}}(e^{c+\beta\gamma\mathsf{t}}z_0, \mathsf{t}w_0)}{i\partial_2 P(e^{c+\beta\gamma\mathsf{t}}z_0, \mathsf{t}w_0)\mathsf{t}w_0} \quad (62)
$$

where $(z_0, w_0)$ are zeros of the characteristic polynomial $P(e^{c+\beta\gamma\mathsf{t}}\cdot, \mathsf{t}\cdot)$ on the unit torus. When multiplied by $\mathsf{K}_{\mathbf{e}}$, the numerator is the length of the dual edge $\mathbf{e}^*$ in the natural application from the dual graph $G^*$ to $\mathbb{R}^2$ described below while the denominator is that of the vertical side of the fundamental domain.

*Lemma 3 ([3]).* Let $(e^{B_x}z_0, e^{B_y}w_0)$ be a root of the characteristic polynomial, with $(z_0, w_0)$ on the unit torus. The 1-form

$$
\mathbf{e} = (\mathbf{w}, \mathbf{b}) \mapsto iK_{\mathbf{wb}}(e^{B_x}z_0, e^{B_y}w_0)Q_{\mathbf{bw}}(e^{B_x}z_0, e^{B_y}w_0) \quad (63)
$$

19

*is a divergence-free flow. Its dual is therefore the gradient of a mapping from $G^*$ to $\mathbb{R}^2 \simeq \mathbb{C}$.*

*This mapping $\Psi^*$ is $\mathbb{Z}^2$-periodic and the symmetries of its range are generated by*

$$\hat{x} = ie^{B_x} z_0 \partial_1 P(e^{B_x} z_0, e^{B_y} w_0) \ and \ \hat{y} = ie^{B_y} w_0 \partial_2 P(e^{B_x} z_0, e^{B_y} w_0).$$

This application $\Psi$ coincide with the notion of isoradial embedding for dimer models with critical weights (see [7]) and gives a geometry well-adapted for the study of liquid measures on dimer configurations (see for example [3]).

Proposition 1 shows that the kernel giving the correlations has the same form as the original bead model. However, in order to recover the bead model, one can not just look at one type of edges on threads but at all of them.

Since the frozen paths have been chosen to cross no dimer when the slope is on the side of the particular Newton polygon we are looking at, they are bordered by white vertices on their left, and black vertices on their right. For a reason of parity between white and black vertices, there is no dimer configuration of the graph $G_1$ deprived of the projection of these two vertices having a height change[2] on the side of $N(P)$. Therefore the arguments of the proof of proposition 1 can be applied to obtain similar asymptotics as those given in that proposition for the coefficients of $\mathsf{K}_{\gamma,\mathsf{t}}^{-1}$ between these vertices.

**Proposition 2.** *Let $\mathbf{b}_{x,y}$ and $\mathbf{w}$ be respectively a black and a white vertex each bordering one of these paths, and in fundamental domains separated by a lattice translation $(x,y)$. In the scaling limit*

$$\mathsf{t} \to 0, \quad \mathsf{t}\beta y\sqrt{1-\gamma^2} \to \xi, \tag{64}$$

*the coefficient $\mathsf{K}_{\gamma,\mathsf{t}}^{-1}(\mathbf{b}_{x,y}, \mathbf{w})$ has the following asymptotics*

$$\mathsf{K}_{\gamma,\mathsf{t}}^{-1}(\mathbf{b}_{x,y}, \mathbf{w}) \sim \mathsf{t}\rho_{\mathbf{bw}} J_\gamma(x, \xi), \tag{65}$$

*where*

$$\rho_{\mathbf{bw}} = \frac{\partial_2 Q_{\mathbf{bw}}(e^c, 0)}{\partial_2 P(e^c, 0)}. \tag{66}$$

These coefficients $\rho_{\mathbf{bw}}$ are in fact the product of two terms, one depending only on $\mathbf{b}$ and the other on $\mathbf{w}$. This property is stated in the following lemma

**Lemma 4.** *The rank of the matrix $\partial_2 Q(e^c, 0)$, restricted to projections of vertices bordering a thread, is equal to 1. In particular, for any $\mathbf{b}$ and any $\mathbf{w}$ bordering a thread, there exist $U_{\mathbf{b}}$ and $V_{\mathbf{w}}$ such that*

$$\rho_{\mathbf{bw}} = U_{\mathbf{b}} V_{\mathbf{w}}. \tag{67}$$

*Proof.* The matrix $\partial_2 Q(e^c, 0)$ is the limit when $\mathsf{t}$ goes to zero of

$$\frac{1}{\mathsf{t}w_0} Q(e^{c+\beta\gamma\mathsf{t}} z_0, \mathsf{t}w_0) \tag{68}$$

---

[2]The term *height change* here is an abuse of notations, since the difference between the reference unit flow $\mathcal{C}_0$ and the one corresponding to any dimer configuration of $G_1$ deprived of the two vertices has a non-zero divergence. What we mean here by this expression is in fact the powers in $z$ and $w$ in the weight of the configuration computed using the magnetically altered Kasteleyn operator $K(z,w)$ divided by that of the reference dimer configuration.

where $(z_0, w_0)$ are zeros on the unit torus of $P(e^{c+\beta\gamma\mathtt{t}}z, \mathtt{t}w)$. These zeros depend on $\mathtt{t}$ and $\gamma$ and their the first term in their expansion in $\mathtt{t}$ is obtained by plugging $\phi = \pm 1$ into equations (50) and (51):

$$z_0 = 1 + O(\mathtt{t}), \quad w_0 = \gamma \pm i\sqrt{1 - \gamma^2} + O(\mathtt{t}). \tag{69}$$

Since $(e^{c+\beta\gamma\mathtt{t}}z_0, \mathtt{t}w_0)$ is not real, it is a simple zero of $P = \det K$, since the mapping from the spectral curve to its amœba is 2-to-1 out of the real locus. $Q$ is the comatrix of $K$, its rank is 1 at a simple zero of $P$. Therefore, as the limit of sequence of rank 1 matrices, the matrix $\partial_2 Q(e^c, 0)$ has a rank a most 1. As there is at least an non-zero entry in this matrix, the rank is equal to 1.

The coefficient $\rho_{\mathbf{bw}}$ is a multiple of the entry $(\mathbf{b}, \mathbf{w})$ of this matrix. Its decomposition into a product comes from the representation of a rank-1 matrix as a tensor product of a vector and a linear form. $\square$

## 5.4 Convergence to the bead model

We already said that the threads of our bead model would be the infinite collection of vertical paths, translated one from another, that are frozen, *i.e* they do not cross any dimer when the slope of the measure lies on the boundary of the Newton polygon. The beads are represented by the dimers crossing these paths when the magnetic field lies in one of the vertical tentacles of the amœba.

Like in section 3, as the magnetic field goes deeper into the tentacle of the amœba, the picture of the graph in the plane is rescaled in such a way that although the probability of seeing a dimer crossing these "almost-frozen" paths goes to zero, the average number of such edges by centimeter of thread stays almost constant. The scaling limit we perform is

$$\mathtt{t} \to 0, \qquad \mathtt{t}\beta y\sqrt{1 - \gamma^2} \to \xi \in \mathbb{R}. \tag{70}$$

To find the limiting distribution of this beads, we first evaluate the quantities

$$\mathbb{E}\left[\frac{X_{I_1}!}{(X_{I_1} - n_1)!} \cdots \frac{X_{I_k}!}{(X_{I_k} - n_k)!}\right] \tag{71}$$

where $X_{I_j}$ is the number of dimers crossing the (rescaled) thread interval. We look in details at the case $k = 1$ when only one thread interval is at stake. The other cases are similar. For a given $n$, and a fixed value of $\gamma$ and of the scaling parameter $\mathtt{t}$, we have

$$\mathbb{E}_{\gamma,\mathtt{t}}\left[\frac{X_I!}{(X_I - n)!}\right] = \sum_{\substack{\mathbf{e}_1,\ldots,\mathbf{e}_n \in I \\ \text{distinct}}} \mathbb{P}_{\gamma,\mathtt{t}}[\mathbf{e}_1, \ldots, \mathbf{e}_n \in \mathcal{C}] \tag{72}$$

where the sum is over all possible $n$-tuples of edges crossing the thread interval $I$. The edges crossing $I$ are labeled by their type (*i.e.* their projection on $G_1 = G/\mathbb{Z}^2$) and the coordinates of the fundamental domain they belong to. The edge $\mathbf{e}_{\mathbf{x}}^j$ represents the edge of type $j$ in the fundamental domain with coordinates $\mathbf{x} = (x, y)$. The type label $j$ ranges from 1 to $d$. Since the probability of having two such edges in the same fundamental domain is negligible, we can rewrite this sum of probabilities, as a sum over the fundamental domains and the types of edges crossing the thread interval.

$$\mathbb{E}_{\gamma,\mathtt{t}}\left[\frac{X_I!}{(X_I - n)!}\right] = \sum_{\substack{\mathbf{x}_1,\ldots,\mathbf{x}_n \in I \\ \text{distinct}}} \sum_{j_1,\ldots,j_n=1}^{n} \mathbb{P}_{\gamma,\mathtt{t}}\left[\mathbf{e}_{\mathbf{x}_1}^{j_1}, \ldots, \mathbf{e}_{\mathbf{x}_n}^{j_n} \in \mathcal{C}\right] + O(\mathtt{t}) \tag{73}$$

21

The different probabilities $\mathbb{P}_{\gamma,\mathsf{t}}\left[\mathbf{e}_{\mathbf{x}_1}^{j_1},\ldots,\mathbf{e}_{\mathbf{x}_n}^{j_n}\in\mathcal{C}\right]$ are given by the determinant of a $n\times n$ matrix that is equal to

$$(\mathsf{t}\beta\sqrt{1-\gamma^2})^n\left(\prod_{l=1}^{n}\mathsf{K}_{j_l}\right)\times\det_{1\le k,l\le n}\left[\rho_{j_k j_l}J_\gamma(x_k-x_l,\mathsf{t}\beta\sqrt{1-\gamma^2}(y_k-y_l))\right]+O(\mathsf{t}^{n+1})\qquad(74)$$

Since $\rho_{jk}$ is the product of two terms $U_j V_k$, by carrying out of the determinant by $n$-linearity these coefficients, equation (74) becomes

$$(\mathsf{t}\beta\sqrt{1-\gamma^2})^n\left(\prod_{l=1}^{n}\mathsf{K}_{j_l}\right)\times\det_{1\le k,l\le n}\left[U_{j_k}V_{j_l}J_\gamma(x_k-x_l,\mathsf{t}\beta\sqrt{1-\gamma^2}(y_k-y_l))\right]+O(\mathsf{t}^{n+1})=$$

$$(\mathsf{t}\beta\sqrt{1-\gamma^2})^n\left(\prod_{l=1}^{n}\mathsf{K}_{j_l}U_{j_l}V_{j_l}\right)\times\det_{1\le k,l\le n}\left[J_\gamma(x_k-x_l,\mathsf{t}\beta\sqrt{1-\gamma^2}(y_k-y_l))\right]+O(\mathsf{t}^{n+1})=$$

$$(\mathsf{t}\beta\sqrt{1-\gamma^2})^n\left(\prod_{l=1}^{n}\mathsf{K}_{j_l}\rho_{j_l}\right)\times\det_{1\le k,l\le n}\left[J_\gamma(x_k-x_l,\mathsf{t}\beta\sqrt{1-\gamma^2}(y_k-y_l))\right]+O(\mathsf{t}^{n+1})\quad(75)$$

Summing now over the different types of edges, one gets

$$\sum_{j_1,\ldots,j_n=1}^{d}\mathbb{P}_{\gamma,\mathsf{t}}\left[\mathbf{e}_{\mathbf{x}_1}^{j_1},\ldots,\mathbf{e}_{\mathbf{x}_n}^{j_n}\in\mathcal{C}\right]=$$

$$(\mathsf{t}\beta\sqrt{1-\gamma^2})^n\left(\sum_{j=1}^{d}\mathsf{K}_{j_l}\rho_{j_l}\right)^n\det_{1\le k,l\le n}\left[J_\gamma(x_k-x_l,\mathsf{t}\beta\sqrt{1-\gamma^2}(y_k-y_l))\right]+O(\mathsf{t}^{n+1})\quad(76)$$

$\mathsf{K}_j\rho_j$ is the proportion of edges of type $j$ along the thread. These coefficients sum up to 1, and we have finally that expression (73) is a Riemann sum for

$$\int\cdots\int_{I^n}\det_{1\le k,l\le n}\left[J_\gamma(x_k-x_l,\xi_k-\xi_l)\right]\mathrm{d}^n\xi\qquad(77)$$

and the same argument of domination as in the proof of theorem 2 implies that the distribution of $X_I$ converges to the distribution of beads in the interval $I$ in the bead model of parameter $\gamma$. The generalization to any finite dimensional distribution is notationally cumbersome, but straightforward. These considerations give thus the proof of the following theorem

**Theorem 3.** *Let $\gamma\in(-1,1)$. In the scaling limit $\mathsf{t}\to 0$, $\mathsf{t}\beta y\sqrt{1-\gamma^2}\to\xi$, the point process describing the position of rare edges on the threads, identified with the almost frozen paths converges to the* bead model *of index $\gamma$, i.e. the determinantal point process on $\mathbb{Z}\times\mathbb{R}$ with kernel $J_\gamma$.*

Recall that $\gamma$ describes the different possible ways to go deep into a tentacle. This theorem states that the bead model, with its 1-parameter family of Gibbs measures, is the universal limiting behavior of any dimer model on a bipartite periodic planar graph when the order parameters $(B_x,B_y)$ go to infinity in staying in the liquid phase.
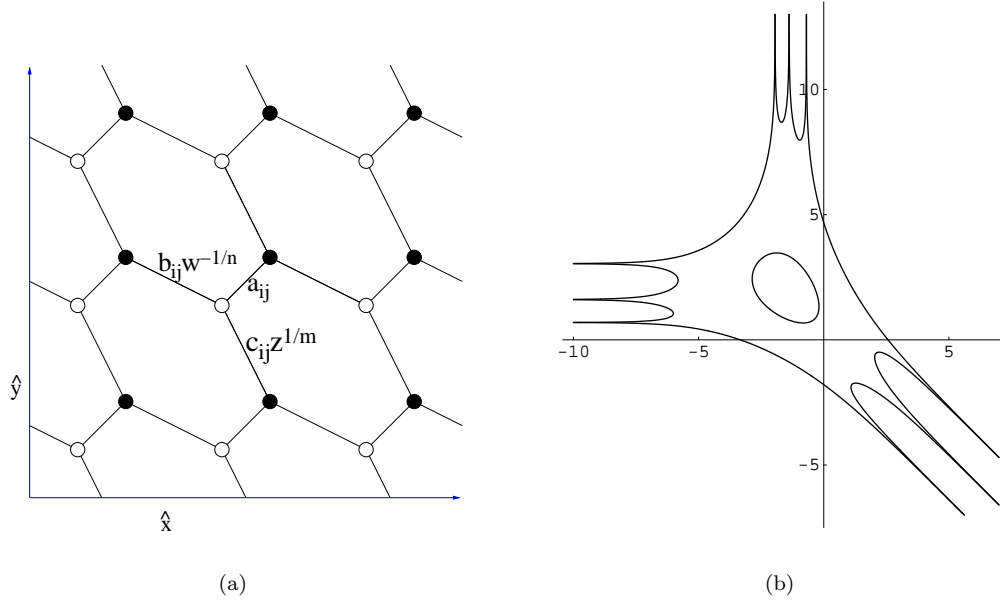
(a)                                                    (b)

Figure 7: (a) A $3 \times 3$ fundamental domain of the honeycomb lattice. Weights of edges around white vertex $\mathbf{w}_{ij}$ are $a_{ij}$, $b_{ij}$ and $c_{ij}$. The Fourier multipliers have been distributed over the edges by gauge transformation. (b) The amœba for generic weights on the graph represented on the left panel. This amœba presents a gaseous phase, and three tentacles in three directions, each corresponding to a collection of frozen paths drawn on figure 8.

# 6    Interaction between bead models

It often happens that a side of the Newton polygon is not the result of a unique frozen path, but that different paths give the same constraint on the slope. In that case, we do not have just one family of frozen paths, but several parallel families of thread, carrying all in the scaling limit a bead model. In this section, we describe the interaction between these different bead models in the case of the generic case of the honeycomb lattice $H$ with a $n \times m$ fundamental domain.

The fundamental domain of this periodic planar graph is represented on figure 7 for $n = m = 3$. The vertices of the quotient $H_1$ by the action of $\mathbb{Z}^2$ by translation are labeled by two integers, $i$ and $j$ ranging respectively from 1 to $n$, and from 1 to $m$. The weights of the edges around the white vertex labeled by $(i, j)$ are denoted by $a_{ij}$, $b_{ij}$ and $c_{ij}$. By an appropriate gauge transformation [9], one can spread the factors $z$ and $w$ in the magnetically altered Kasteleyn matrix $K(z, w)$ so that the coefficients of this operator are $a_{ij}$, $b_{ij}w^{-1/n}$ and $c_{ij}z^{1/m}$. The reference dimer configuration we will use is the configuration containing $a$-edges.

One distinguishes three special classes of dual cycles in $G_1$, say $\mathbf{A}$, $\mathbf{B}$ and $\mathbf{C}$ that cross only edges of a given type (respectively $a$, $b$ and $c$). The lifts of these classes to $H$ are represented on figure 8. The $\mathbf{B}$ class is constituted by $n$ vertical straight paths with homology class $(0, 1)$, whereas the $\mathbf{C}$ class contains the $m$ horizontal straight paths with homology class $(1, 0)$. The $\mathbf{A}$ class contains $d = \gcd(n, m)$ paths with homology $(\frac{m}{d}, \frac{n}{d})$. The three classes of cycles lift to $H$, forming three

23

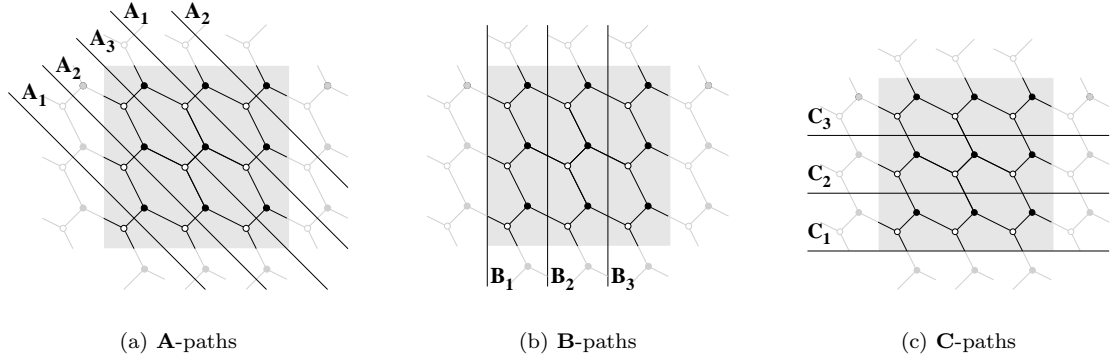(a) **A**-paths       (b) **B**-paths       (c) **C**-paths

Figure 8: the three classes of possible frozen paths: **A**, **B** and **C**.

classes of parallel families of straight lines.

The Newton polygon of the weighted dimer graph $G$ is a right triangle. Each side of the triangle corresponds to Gibbs measures for which all the paths of one of the three classes are frozen. The horizontal side contains $n + 1$ lattice points. The amœba of the associated spectral curve exhibits $n$ vertical tentacles separating $n + 1$ unbounded complementary components – solid phases in the phase diagram – each corresponding to a lattice point of the horizontal side.

The frozen configurations are obtained as follows: when the Gibbs measure's slope lies, say, on the horizontal side of the Newton polygon, there is almost surely no edge crossing the **B** class of paths. These paths delimit thin strips where one sees either an infinite succession of $a$-edges or an infinite collection of $c$-edges. On $G_1$ and in presence of a magnetic field $(B_x, B_y)$, the associated patterns have weights $\prod_{i=1}^{m} a_{ij}$ and $e^{B_x} \prod_{i=1}^{m} c_{ij}$. The patterns with the highest weight correspond to the type of columns appearing in the configuration with probability 1. When the horizontal component of the magnetic field is very negative, the weight of the '$a$' patterns are greater than the '$c$' ones, but as $B_x$ increases, the weight of the second pattern becomes more important, and at some point, it becomes bigger that the first one. In the graph $G$ the $a$-edges that were filling the space between the two **B** paths switch to $c$-edges. Generically the values of $B_x$ corresponding to such a switch are all different. They correspond to the abscissæ of the vertical tentacles of the amœba.

In a fixed window and when $B_y$ is very large, one sees columns of edges of the same type ($a$, or $c$) with a probability close to 1. When the magnetic field lies in a tentacle of the phase diagram, the system hesitates between two states for a given type of columns. With a probability $p$ bounded away from 0 and 1, the column is filled with $a$-edges, and with probability $1 - p$, it is filled with $c$-edges. If one rescales vertically the graph in the same time as $B_y$ goes to $+\infty$, then one will be able to see the transition between these two possibilities: between the two types of fillings, a $b$-edge is inserted. The edge creates a defect in the neighboring column that is supposed to be frozen. This discussion is quantified in the following proposition:

**Proposition 3.** *If*

$$B_x < \sum_{i=1}^{m} \log \frac{a_{ij_0}}{c_{ij_0}}, \tag{78}$$

24

*then with probability going to 1 when $B_y$ goes to infinity, the columns of type $j_0$ will be filled with a-edges.*

*If the inequality is strict in the other direction, then they will be filled with c-edges with probability going to 1 when $B_y$ goes to infinity.*

*Proof.* When the vertical component of the magnetic field is very negative, the main contribution to the characteristic polynomial is given by the configurations on $G_1$ that contain no b-edges. One can choose to fill each strip of $G_1$ between two consecutive frozen cycles either by a-edges or by c-edges. Choosing a filling with c edges induces a height change of $m$ in the vertical direction. Therefore

$$P^B(z,w) = P(e^{B_x}z, e^{B_y}w) = \prod_{j=1}^{n} \left( \prod_{i=1}^{m} a_{ij} - (-1)^m e^{B_x} z \prod_{i=1}^{m} c_{ij} \right) + O(\mathtt{t}) \tag{79}$$

where $\mathtt{t} = e^{B_y}$ is small.

Let $\mathbf{b}$ and $\mathbf{w}$ two vertices in the same strip $j_0$ in $G_1$. Denote by $\mathbf{b}_y$ and $\mathbf{w}_0$ lifts of $\mathbf{b}$ and $\mathbf{w}$ in the same column of $G$, separated by $y$ fundamental domains. The entry of the inverse Kasteleyn operator between these two vertices is easily evaluated: recall that $Q_{\mathbf{bw}}$ is the characteristic polynomial of the graph $G$ where all the translated of $\mathbf{b}$ and $\mathbf{w}$, as well as all the edges connected to these vertices, have been removed. Repeating the argument given above, we find the main contribution to it,

$$Q_{\mathbf{bw}}^B(z,w) = Q_{\mathbf{bw}}(e^{B_x}z, e^{B_y}w) = M_{\mathbf{bw}} z^\delta \prod_{\substack{j=1 \\ j \neq j_0}}^{n} \left( \prod_{i=1}^{m} a_{ij} - (-1)^m e^{B_x} z \prod_{i=1}^{m} c_{ij} \right) + O(\mathtt{t}) \tag{80}$$

where $M_{\mathbf{bw}} z^\delta$ is the weight of the dimer configuration of the strip $j_0$ of $G_1$ deprived of $\mathbf{b}$ and $\mathbf{w}$. The coefficient of the inverse Kasteleyn operator corresponding to these two vertices whose fundamental domains are separated by the lattice vector $(x, y)$ is given by

$$\mathsf{K}_B^{-1}(\mathbf{b}_y, \mathbf{w}_0) = \iint_{\mathbb{T}^2} \frac{z^{-y} w^0 Q_{\mathbf{bw}}^B(z,w)}{P^B(z,w)} \frac{dz}{2i\pi z} \frac{dw}{2i\pi w} \tag{81}$$

$$= \iint_{\mathbb{T}^2} \frac{z^{-y+\delta} M_{\mathbf{bw}}}{\left( \prod_{i=1}^{m} a_{ij_0} - (-1)^m e^{B_x} z \prod_{i=1}^{m} c_{ij_0} \right)} \frac{dz}{2i\pi z} \frac{dw}{2i\pi w} + O(\mathtt{t}) \tag{82}$$

$$= \int_{\mathbb{S}^1} \frac{z^{-y+\delta} M_{\mathbf{bw}}}{\left( \prod_{i=1}^{m} a_{ij_0} - (-1)^m e^{B_x} z \prod_{i=1}^{m} c_{ij_0} \right)} \frac{dz}{2i\pi z} + O(\mathtt{t}) \tag{83}$$

Suppose that $B_x < \sum_{i=1}^{m} \log \frac{a_{ij_0}}{c_{ij_0}}$, the other case is similar. In that case, the pole located at

$$z = (-1)^m \frac{\prod_{i=1}^{m} a_{ij_0}}{e^{B_x} \prod_{i=1}^{m} c_{ij_0}} \tag{84}$$

is outside of the unit disk. If $y - \delta < 0$, then there is no pole at all in the unit disk, and therefore the integral over $z$ is zero. However, if $y - \delta \geq 0$, then the integral equals the opposite of the residue at $z_0$, and

$$\mathsf{K}_B^{-1}(\mathbf{b}_y, \mathbf{w}_0) = \frac{M_{\mathbf{bw}}}{(-1)^m e^{B_x} \prod_{i=1}^{m} c_{ij_0}} \left( \frac{\prod_{i=1}^{m} a_{ij_0}}{(-1)^m e^{B_x} \prod_{i=1}^{m} c_{ij_0}} \right)^{-y-1} + O(\mathtt{t}) \tag{85}$$

25

When $\mathbf{b}_y$ and $\mathbf{w}_0$ are the ends of an edge with weight $a_{i_0 j_0}$, $M_{\mathbf{bw}} = \prod_{i \neq i_0} a_{i j_0}$ and $y$ and $\delta$ equal 0. It follows that

$$\mathsf{K}_B^{-1}(\mathbf{b}_y, \mathbf{w}_0) = \frac{M_{\mathbf{bw}}}{\prod_{i=1}^m a_{i j_0}} + O(\mathsf{t}) = \frac{1}{a_{i_0 j_0}} + O(\mathsf{t}) \tag{86}$$

Thus, the probability of this $a$-edge, given by $a_{i_0 j_0} \mathsf{K}_B^{-1}(\mathbf{b}_y, \mathbf{w}_0)$ goes to 1 when $\mathsf{t}$ goes to zero.

On the other hand, in the case when $\mathbf{b}$ and $\mathbf{w}$ are the ends of a 'c'-type edge, then either $y = -1$ or $\delta = 1$. In both cases, $\mathsf{K}_B^{-1}(\mathbf{b}_y, \mathbf{w}_0)$ is $O(\mathsf{t})$. Thus the probability of this edge goes to zero when $\mathsf{t}$ goes to zero. Such an edge is called *non typical*. $\qquad\square$

A sequence of non-typical edges in a frozen column is initiated by the presence of a bead (a 'b'-edge) crossing a neighboring wire. The analysis we made of the inverse Kasteleyn operator allows us to determine the distribution of the sequence of non typical edges in a frozen column.

**Proposition 4.** *The length of a succession of non typical edges in a frozen column has a geometric distribution. The parameter of the geometric distribution has an explicit expression in terms of ratios of lengths of dual edges.*

*Proof.* We suppose that in the frozen column $j_0$, we only see $a$-edges with probability close to 1. The following inequality

$$B_x < \sum_{i=1}^m \log \frac{a_{i j_0}}{c_{i j_0}} \tag{87}$$

is satisfied. Since we work only in one column, we will drop the index $j_0$ for the sake of simplicity. Given that the edge $\mathbf{e} = (\mathbf{w}, \mathbf{b})$ with weight $b_{i_0}$ is present in the dimer configuration, we compute the probability of seeing $N$ successive $c$-edges after this bead. Denote by $\mathbf{e}_1^c = (\mathbf{w}_1, \mathbf{b}_1), \ldots, \mathbf{e}_N^c(\mathbf{w}_N, \mathbf{b}_N)$ the $N$ $c$-edges. The weights of the edges around vertex $\mathbf{w}_i$ are $a_{[i]}, b_{[i]}, c_{[i]}$, where $[i] = (i_0 + i \mod m) + 1$. The conditional probability we want to compute is give by the following formula

$$\mathbb{P}\left[\mathbf{e} \in \mathcal{C} \text{ and } \forall i = 1, \ldots, N \; \mathbf{e}_i^c \in \mathcal{C} \;\middle|\; \mathbf{e} \in \mathcal{C}\right] =$$

$$\frac{\mathbb{P}\left[\mathbf{e} \in \mathcal{C} \text{ and } \forall i = 1, \ldots, N \; \mathbf{e}_i^c \in \mathcal{C}\right]}{\mathbb{P}\left[\mathbf{e} \in \mathcal{C}\right]} = \left(\prod_{i=1}^N c_{[i]}\right) \frac{\det A_{N+1}}{\mathsf{K}^{-1}(\mathbf{b}, \mathbf{w})} \tag{88}$$

where $A_{N+1}$ is the following square matrix whose entries are inverse Kasteleyn operator coefficients:

$$A = \begin{bmatrix} \mathsf{K}^{-1}(\mathbf{b}, \mathbf{w}) & \cdots & \mathsf{K}^{-1}(\mathbf{b}_j, \mathbf{w}) & \cdots \\ \vdots & \ddots & \vdots & \\ \mathsf{K}^{-1}(\mathbf{b}, \mathbf{w}_i) & & \mathsf{K}^{-1}(\mathbf{b}_j, \mathbf{w}_i) & \\ \vdots & & \vdots & \ddots \end{bmatrix} \tag{89}$$

Since $\mathbf{w}$ and the white vertices $\mathbf{w}_i$ stand on different sides of a frozen path, the associated coefficients $\mathsf{K}^{-1}(\mathbf{b}, \mathbf{w}_i)$ are $O(\mathsf{t})$. More precisely, from (65), one has

$$\mathsf{K}^{-1}(\mathbf{b}, \mathbf{w}_i) = \mathsf{t} \rho_{\mathbf{bw}_i} + O(t^2). \tag{90}$$

Besides, if $i \leq j$, the power of $z$ in the numerator of (81) is positive, and it follows from computations made above that $\mathsf{K}^{-1}(\mathbf{b}_j, \mathbf{w}_i)$ is also $O(\mathsf{t})$.

26

For $i \in \{1, \dots, N\}$ and with the convention that $\mathbf{w}_0 = \mathbf{w}$, $\mathbf{w}_{i-1}$ and $\mathbf{b}_i$ are the ends of an $a$-edge with weight $a_{[i-1]}$. The same computations as above show that $\mathsf{K}^{-1}(\mathbf{b}_i, \mathbf{w}_{i-1}) = \frac{1}{a_{[i-1]}}$. As a consequence, the asymptotic expansion of the determinant of $A_{N+1}$ is given by the product of these elements just above the diagonal times the last element of the first column.

$$\det A_{N+1} = \mathsf{t} \rho_{\mathbf{bw}_N} \prod_{i=1}^{N} \frac{1}{a_{[i-1]}} + O(\mathsf{t}^2) \tag{91}$$

As the probability of the bead is $b_{i_0} \rho_{\mathbf{bw}} \mathsf{t} + O(\mathsf{t}^2)$, the conditional probability we want is given by

$$\mathbb{P}\left[N \text{ successive } c\text{-edges} \,|\, \text{bead}\right] = \frac{\rho_{\mathbf{bw}}}{\rho_{\mathbf{bw}_N}} \prod_{i=1}^{N} \frac{c_{[i]}}{a_{[i-1]}} + O(\mathsf{t}) \tag{92}$$

Using proposition 4, one can rewrite $\rho_{\mathbf{bw}_N}/\rho_{\mathbf{bw}}$ as the following telescopic product

$$\frac{\rho_{\mathbf{bw}_N}}{\rho_{\mathbf{bw}}} = \frac{U_{\mathbf{b}} V_{\mathbf{w}_N}}{U_{\mathbf{b}} V_{\mathbf{w}}} = \prod_{i=1}^{N} \frac{U_{\mathbf{b}_i} V_{\mathbf{w}_i}}{U_{\mathbf{b}_i} V_{\mathbf{w}_{i-1}}}. \tag{93}$$

Plugging this into (92), one gets

$$\mathbb{P}\left[N \text{ successive } c\text{-edges} \,|\, \text{bead}\right] = \prod_{i=1}^{N} \frac{c_{[i]} U_{\mathbf{b}_i} V_{\mathbf{w}_i}}{a_{[i-1]} U_{\mathbf{b}_i} V_{\mathbf{w}_{i-1}}} + O(\mathsf{t}) = \prod_{i=1}^{N} \frac{\ell(c_{[i]})}{\ell(a_{[i-1]})} + O(\mathsf{t}) \tag{94}$$

where $\ell(a_{[i-1]})$ and $\ell(c_{[i]})$ are respectively the length of the dual edges with weight $a_{[i-1]}$ and $c_{[i]}$ given by the mapping described in lemma 3. In particular, in the limit $\mathsf{t} \to 0$, the probability that the length $L$ of this succession of non typical edges exceeds $p$ fundamental domains equals

$$\mathbb{P}\left[L \geq p\right] = \left(\prod_{i=1}^{m} \frac{\ell(c_i)}{\ell(a_i)}\right)^p. \tag{95}$$

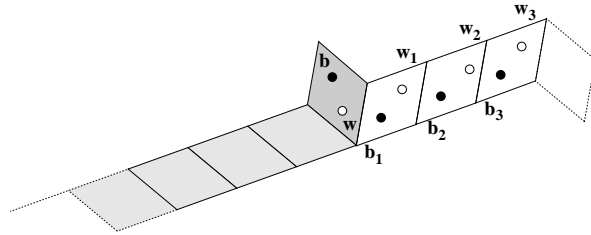Thus, in the limit, $L$ has a geometric distribution. $\qquad\square$



Figure 9: Illustration of proposition 4. Here is represented a frozen column of (horizontal) $a$-rhombi, perturbed by the presence of a defect (the $b$-rhombus corresponding to the edge $(\mathbf{w}, \mathbf{b})$), followed by a finite sequence of $c$-rhombi.

Pushing further the above computations of the lengths of the non typical sequences of edges in frozen columns, one can derive the following:

**Proposition 5.** *The limiting bead models on the different families of threads $\mathbf{B}_j$ are perfectly correlated: the distance between beads on each side of a frozen column converges in probability to zero.*

*Proof.* The details of the proof are omitted here, but by looking carefully at the determinants in the proof given above, one can in fact see that, for every $\mathtt{t}$, the probability that a sequence of non typical edges in a frozen columns exceeds, say, $\frac{1}{\sqrt{\mathtt{t}}}$ is of order $q^{1/\sqrt{\mathtt{t}}}$, and thus decays very fast when $\mathtt{t}$ goes to zero. Thus, in the vertically rescaled graph, the distance between two beads at the extremity of a sequence of non typical edges is close to 0. In the scaling limit, the distance between these beads converges in probability to 0. □

As a consequence, the picture of a typical dimer configuration for a Gibbs measure corresponding to a point in a tentacle of the phase diagram looks like the figure 10.
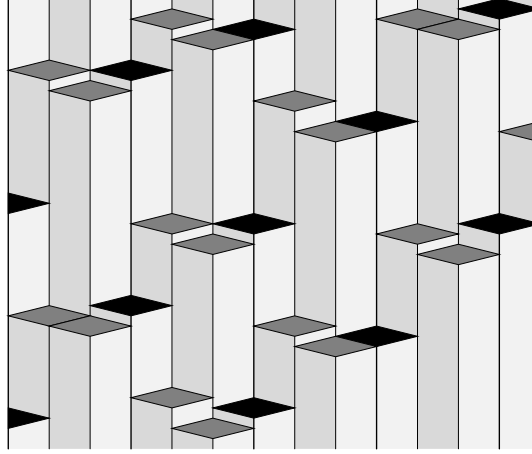


Figure 10: A sketch of a typical tiling for a Gibbs measure corresponding to a point inside a tentacle. The black beads mark the transition between the two dominant type of edges. Next to them, beads also appear on the other threads to compensate the defect created in frozen columns.

# Acknoledgments

# References

[1] J. Baik, T. Kriecherbauer, K. D. T.-R. McLaughlin, and P. D. Miller, *Uniform asymptotics for polynomials orthogonal with respect to a general class of discrete weights and universality results for associated ensembles: announcement of results*, Int. Math. Res. Not., (2003), pp. 821–858.

[2] Y. Baryshnikov, *GUEs and queues*, Probab. Theory Related Fields, 119 (2001), pp. 256–274.

[3] C. Boutillier, *Pattern densities in fluid dimer models*, (2006).

[4] D. J. Daley and D. Vere-Jones, *An introduction to the theory of point processes*, Springer Series in Statistics, Springer-Verlag, New York, 1988.

[5] K. Johansson, *Non-intersecting paths, random tilings and random matrices*, Probab. Theory Related Fields, 123 (2002), pp. 225–280.

[6] R. Kenyon, *Local statistics of lattice dimers*, Ann. Inst. H. Poincaré Probab. Statist., 33 (1997), pp. 591–618.

[7] ———, *The Laplacian and Dirac operators on critical planar graphs*, Invent. Math., 150 (2002), pp. 409–439.

[8] R. Kenyon and A. Okounkov, *Planar dimers and Harnack curves*, (2003).

[9] R. Kenyon, A. Okounkov, and S. Sheffield, *Dimers and amoebae*, (2003).

[10] M. L. Mehta, *Random matrices*, vol. 142 of Pure and Applied Mathematics (Amsterdam), Elsevier/Academic Press, Amsterdam, third ed., 2004.

[11] G. Mikhalkin, *Amoebas of algebraic varieties and tropical geometry*, in Different faces of geometry, Int. Math. Ser. (N. Y.), Kluwer/Plenum, New York, 2004, pp. 257–300.

[12] G. Mikhalkin and H. Rullgård, *Amoebas of maximal area*, Internat. Math. Res. Notices, (2001), pp. 441–451.

[13] M. Passare and H. Rullgård, *Amoebas, Monge-Ampère measures, and triangulations of the Newton polytope*, Duke Math. J., 121 (2004), pp. 481–507.

[14] M. Prähofer and H. Spohn, *Current fluctuations for the totally asymmetric simple exclusion process*, in In and out of equilibrium (Mambucaba, 2000), vol. 51 of Progr. Probab., Birkhäuser Boston, Boston, MA, 2002, pp. 185–204.

[15] S. Sheffield, *Random Surfaces: Large Deviations Principles and Gradient Gibbs Measure Classifications* , PhD thesis, Stanford University, 2004.

[16] A. Soshnikov, *Determinantal random point fields*, Uspekhi Mat. Nauk, 55 (2000), pp. 107–160.